NASA/CR—2001-210894 ARL–CR–467

Computerized Design, Generation, and Simulation of Meshing and Contact of Face-Milled Formate Cut Spiral Bevel Gears

Faydor L. Litvin, Qi Fan, and Alfonso Fuentes
University of Illinois at Chicago, Chicago, Illinois

DISTRIBUTION STATEMENT A
Approved for Public Release
Distribution Unlimited

20010611 076

May 2001

The NASA STI Program Office . . . in Profile

Since its founding, NASA has been dedicated to the advancement of aeronautics and space science. The NASA Scientific and Technical Information (STI) Program Office plays a key part in helping NASA maintain this important role.

The NASA STI Program Office is operated by Langley Research Center, the Lead Center for NASA's scientific and technical information. The NASA STI Program Office provides access to the NASA STI Database, the largest collection of aeronautical and space science STI in the world. The Program Office is also NASA's institutional mechanism for disseminating the results of its research and development activities. These results are published by NASA in the NASA STI Report Series, which includes the following report types:

- TECHNICAL PUBLICATION. Reports of completed research or a major significant phase of research that present the results of NASA programs and include extensive data or theoretical analysis. Includes compilations of significant scientific and technical data and information deemed to be of continuing reference value. NASA's counterpart of peer-reviewed formal professional papers but has less stringent limitations on manuscript length and extent of graphic presentations.

- TECHNICAL MEMORANDUM. Scientific and technical findings that are preliminary or of specialized interest, e.g., quick release reports, working papers, and bibliographies that contain minimal annotation. Does not contain extensive analysis.

- CONTRACTOR REPORT. Scientific and technical findings by NASA-sponsored contractors and grantees.

- CONFERENCE PUBLICATION. Collected papers from scientific and technical conferences, symposia, seminars, or other meetings sponsored or cosponsored by NASA.

- SPECIAL PUBLICATION. Scientific, technical, or historical information from NASA programs, projects, and missions, often concerned with subjects having substantial public interest.

- TECHNICAL TRANSLATION. English-language translations of foreign scientific and technical material pertinent to NASA's mission.

Specialized services that complement the STI Program Office's diverse offerings include creating custom thesauri, building customized data bases, organizing and publishing research results . . . even providing videos.

For more information about the NASA STI Program Office, see the following:

- Access the NASA STI Program Home Page at ***http://www.sti.nasa.gov***

- E-mail your question via the Internet to help@sti.nasa.gov

- Fax your question to the NASA Access Help Desk at 301–621–0134

- Telephone the NASA Access Help Desk at 301–621–0390

- Write to:
  NASA Access Help Desk
  NASA Center for AeroSpace Information
  7121 Standard Drive
  Hanover, MD 21076

NASA/CR—2001-210894

ARL–CR–467

Computerized Design, Generation, and Simulation of Meshing and Contact of Face-Milled Formate Cut Spiral Bevel Gears

Faydor L. Litvin, Qi Fan, and Alfonso Fuentes
University of Illinois at Chicago, Chicago, Illinois

Prepared under Grant NAG3–2450

National Aeronautics and
Space Administration

Glenn Research Center

May 2001

Available from

NASA Center for Aerospace Information
7121 Standard Drive
Hanover, MD 21076

National Technical Information Service
5285 Port Royal Road
Springfield, VA 22100

Available electronically at http://gltrs.grc.nasa.gov/GLTRS

Computerized Design, Generation, and Simulation of Meshing and Contact of Face-Milled Formate Cut Spiral Bevel Gears

Faydor L. Litvin, Qi Fan, and Alfonso Fuentes
University of Illinois at Chicago
Department of Mechanical Engineering
Gear Research Center
Chicago, Illinois 60607

Abstract

A new approach for design, generation, and computerized simulation of meshing and contact of face-milled, formate cut spiral bevel gears is presented. The purpose is to develop a low noise, stabilized bearing contact for this type of gear drives. The approach proposed is based on application of three procedures that permit in sequence, to provide a longitudinally directed bearing contact, a predesigned parabolic function of transmission errors and limit the shift of bearing contact caused by errors of alignment. The theory developed is illustrated with an example of design and computation.

Nomenclature

α_g	Profile angle of parabolic blade for gear head cutter at mean point M
α_p	Blade angle for straight blade of pinion head cutter
δ	Elastic approach of contacting surfaces
γ_i $(i=1,2)$	Pitch cone angles of pinion $(i=1)$ and gear $(i=2)$, respectively
γ_{m_i} $(i=1,2)$	Machine root angles for pinion $(i=1)$ and gear $(i=2)$, respectively
γ_{r_i} $(i=1,2)$	Root cone angles for pinion $(i=1)$ and gear $(i=2)$, respectively
γ	Shaft angle
η_i $(i=1,2)$	Tangent to the path of contact on the pinion $(i=1)$ and gear $(i=2)$, respectively
θ_p , θ_g	Surface parameters of the pinion and gear head cutters, respectively
λ_f , λ_w	Surface parameters of the pinion and the gear fillet parts of the head cutter
$\sigma^{(ij)}$	Angle formed between principal directions $(i, j,= 1, 2, p, g)$
ϕ_i $(i=1,2)$	Angles of rotation of pinion $(i=1)$ and gear $(i=2)$ in the process of meshing
ψ_{c_1}	Angle of rotation of the cradle in the process for generation of the pinion
ψ_1	Angle of rotation of the pinion in the process for generation
ρ_f , ρ_w	Fillet radii for the pinion and gear
$\boldsymbol{\omega}^{(1)}$	Angular velocity of the pinion (in meshing and generation)
Σ_i $(i=1,2)$	Pinion $(i=1)$ or gear $(i=2)$ tooth surface
Σ_k $(k=p,g)$	Pinion $(k=p)$ or gear $(k=g)$ generating surface
ΔH, ΔD	Pinion and gear axial displacements, respectively
E_{m_1}	Blank offset for pinion
X_{B_1}	Sliding base for pinion
X_{D_1}	Machine center to back for pinion
X_G	Machine center to back for gear

ΔE, $\Delta\gamma$	Errors of the offset and shaft angle, respectively
$\Delta\phi_2(\phi_1)$	Function of transmission errors
a_c	Parabola coefficient of gear head cutter blade
a_{d_1}	Dedendum of pinion
A_m, F_w	Mean cone distance and face width
b_i	Coefficients of modified roll for pinion generation, (i=1, 2, 3)
$\mathbf{e}_f$, $\mathbf{e}_h$, $\mathbf{e}_s$, $\mathbf{e}_q$	Unit vectors of principal directions of pinion and gear tooth surfaces, respectively
$\mathbf{e}_t$, $\mathbf{e}_p$, $\mathbf{e}_g$, $\mathbf{e}_u$	Unit vectors of principal directions of cutter surfaces for pinion and gear, respectively
$k_n^{(i)}$	Normal curvature of surface Σ_i
$k_n^{(r)}$	Relative normal curvature
k_f, k_h, k_s, k_q	Principal curvatures of pinion and gear tooth surfaces, respectively
k_t, k_p, k_g, k_u	Principal curvatures of cutter surfaces for pinion and gear, respectively
L_A, R_A	Cylindrical coordinates for contact point A on gear tooth surface
m_{12}'	Second derivative of transmission function $\phi_2(\phi_1)$
m_{12}	gear ratio
M	Mean contact point
$\mathbf{M}_{ji}$, $\mathbf{L}_{ji}$	Matrix of coordinate transformation from system S_i to system S_j
$\mathbf{n}_i^{(k)}$, $\mathbf{N}_i^{(k)}$	Unit normal and normal to the surface Σ_k represented in coordinate system S_i
N_i (i=1,2)	Tooth number of pinion (i=1) or gear (i=2)
q_1	Installment angle for pinion head cutter
R_p, R_g	Radii of the head-cutter at mean point for the pinion and gear
R_u	Gear cutter radii
$\mathbf{r}_i$	Position vector in system S_i (i =1, 2, b_1, b_2, h, l, m_1, m_2, p, g)
s_p	Surface parameters of the pinion
S_i	Coordinate system (i =1, 2, b_1, b_2, h, l, m_1, m_2, p, g)
S_{r_1}	Radial setting of the head cutter of the pinion
u_g	Gear tooth surface parameter
$\mathbf{v}_r^{(k)}$ (k=p, g)	Velocity of contact point in its motion over surface Σ_k
$\mathbf{v}_{tr}^{(i)}$	Transfer velocity of contact point in its motion with surface Σ_i
$\mathbf{v}^{(ij)}$	Relative velocity of contact point (i, j =1, 2, c_1, p)
$v_s^{(i)}$, $v_q^{(i)}$	Components of the velocity of the contact point in its motion over surface Σ_i
X_f, X_g	Center distances of fillet circular arcs of pinion and gear, respectively
$2a$	Length of major axis of contact ellipse

1. Introduction

Design and generation of spiral bevel gears is a subject of intensive research of scientists, designers and manufacturers [1 - 7]. High quality equipment such as CNC (computer numerically controlled) machines and tools are produced by the Gleason Works (USA) and the Klingelnber-Orlikon (Germany and Switzerland) that manufacture these gears. However, the quality of spiral bevel gears depends substantially on the choice of machine-tool settings that have to be determined for the generation of the gears. The machine-tool settings are not standardized and their determination is the subject of a skilled design. The freedom of choosing various machine-tool settings provide an opportunity for generation of low-noise, stable bearing contact spiral bevel gears.

The subject of this paper is the enhanced design of face-milled formate cut spiral bevel gears. The term "formate cut" means that the gear is held at rest where it is cut by the tool (head-cutter). Thus, the gear tooth surface is a copy of the tool surface that is a surface of revolution. The pinion tooth surface is generated by a head-cutter while the tool and the pinion performed related rotations. The pinion tooth surface is generated as the envelope to the family of the tool (head-cutter) surfaces. The advantage of formate-cut method is the high productivity of gear generation. The main problem of the design of formate-cut spiral bevel gears is the conjugation of tooth surfaces of the gear and the pinion.

The contents of this paper cover the following topics:
(1) Computational procedures of proposed design that provides a longitudinal bearing contact and a predesigned parabolic function of transmission errors, and the ability to investigate the influence of misalignment.

(2) Computer programs and algorithms developed for synthesis and analysis of meshing and contact of gear drives.

The theory developed is illustrated with an example of computerized design of a formate cut gear drive.

2. Basic Ideas of Proposed Approach

Localization of Contact [1, 8]. The contact of pinion-gear tooth surfaces is localized due to the mismatch of generating surfaces (surfaces of the head-cutters) that is achieved by application of different dimensions of the gear-pinion head-cutters.

The generated pinion-gear tooth surfaces are in point contact at every instant, instead of in line contact. The tooth contact under the load is spread over an elliptical area and the bearing contact is formed as a set of contact ellipses. The magnitude and orientation of instantaneous contact ellipse requires information regarding the elastic deformation of tooth surfaces and the principal curvatures and the directions of tooth surfaces at each instantaneous point of their tangency.

It will be shown later that the path of contact on gear tooth surface is oriented longitudinally. Such a path of contact is favorable for the increase of contact ratio (the average number of teeth that are in contact simultaneously), and avoids edge contact and improves the conditions of transfer of meshing where one pair of teeth is changed for the neighboring one.

The TCA (Tooth Contact Analysis) computer program developed by the authors permits simulation of meshing surfaces and the shift of bearing contact caused by errors of alignment [8, 9]. In some cases of design, it may become necessary to adjust the bearing contact - to deviate it from the longitudinal direction - to reduce the shift of bearing contact caused by misalignment.

Application of Parabolic Profiles of Blades of Gear Head-Cutter. We have mentioned above that the gear tooth surface is generated as a copy of the surface of the gear head-cutter. Usually, straight profile blades are applied for the gear head-cutter. Such blades form the head-cutter generating surface as a cone.

Application of parabolic profiles of the blades instead of straight line profiles permits modification of the gear tooth surface in favor of conjugation of pinion-gear tooth surfaces.

Simulation of Meshing. The algorithm of computerized simulation of meshing [8, 9] provides continuous tangency of contacting gear tooth surfaces Σ_1 and Σ_2 as equality of position vectors $\mathbf{r}_h^{(1)} = \mathbf{r}_h^{(2)}$ and unit normals $\mathbf{n}_h^{(1)} = \mathbf{n}_h^{(2)}$. Instead of equality of unit normals to contacting surfaces, collinearity of surface normals may be considered. Position vectors $\mathbf{r}_h^{(i)}$ $(i=1,2)$ and unit normals $\mathbf{n}_h^{(i)}$ $(i=1,2)$ are considered in fixed coordinate system S_h (Fig. 1).

Application of TCA determines the path of contact on the pinion-gear tooth surfaces, dimensions and orientation of instantaneous contact ellipse at each point of contact, the transmission function $\phi_2(\phi_1)$ that relates the angles of rotation of the gear and the pinion, and function $\Delta\phi_2(\phi_1)$ of transmission errors is determined as

$$\Delta\phi_2(\phi_1) = \phi_2(\phi_1) - \frac{N_1}{N_2}\phi_1 \tag{1}$$

where N_1 and N_2 are the numbers of teeth of the pinion and the gear.

Predesign of Parabolic Function of Transmission Errors [8]. The output of TCA for a misaligned gear drive shows that the transmission function $\phi_2(\phi_1)$ is a piecewise discontinuous almost linear function (Fig. 2(a)). The transfer of meshing with the transmission function $\phi_2(\phi_1)$ (Fig. 2(a)) and function $\Delta\phi_2(\phi_1)$ of transmission errors (Fig. 2(b)) is accompanied with the jump of the angular velocity and therefore noise and vibration are inevitable.

The purpose of synthesis of a low-noise gear drive is to transform the transmission function $\phi_2(\phi_1)$ as shown in Fig. 3(a) and obtain a parabolic function of transmission errors shown in Fig. 3(b). The modified function $\Delta\phi_2(\phi_1)$ (Fig. 3(b)) is a continuous one and is determined as

$$\Delta\phi_2^{(1)}(\phi_1) = -a\phi_1^2 \tag{2}$$

where a is the parabola coefficient.

It is important to recognize that the function of transmission errors must be negative and therefore the gear will lag with respect to the pinion. Therefore, the transfer of meshing is accompanied with elastic deformations, and as a result, the gear ratio is increased.

The desired parabolic function of transmission errors is provided by the respective synthesis of the gear drive. The idea of such synthesis is based on the predesign of a parabolic function obtained by application of modified roll during the process of generation. Modified roll is provided by application of nonlinear relations between the angles of rotation of the cradle of the generation machine and the pinion during the process of pinion generation.

The advantage of the predesign of a parabolic function of transmission errors is that such a function is able to absorb the linear discontinuous function of transmission errors caused by misalignment. This is

illustrated by drawings of Fig. 4(a) that shows a linear function $\Delta\phi_2^{(2)}(\phi_1) = b\phi_1$ (Fig. 4(a)). Function $\Delta\phi_2^{(1)}(\phi_1)$ is predesigned and function $\Delta\phi_2^{(2)}(\phi_1)$ is caused by misalignment. The sum of functions $\Delta\phi_2^{(1)}(\phi_1)$ and $\Delta\phi_2^{(2)}(\phi_1)$ is represented in Fig. 4(a) as $\Delta\psi_2(\psi_1) = -a\psi_1^2$. The parabola coefficient a is the same in functions $\Delta\phi_2^{(1)}(\phi_1)$ and $\Delta\psi_2(\psi_1)$.

The figure confirms that: (i) the predesigned parabolic function absorbs indeed linear function $\Delta\phi_2^{(2)}(\phi_1)$, and (ii) the resulting function $\Delta\psi_2(\psi_1)$ is slightly dislocated with respect to origin of $\Delta\phi_2^{(1)}(\phi_1)$, function $\Delta\psi_2(\psi_1)$ is an unsymmetrical one. Parameters c and d of the origin of $\Delta\psi_2(\psi_1)$ are determined as $d = b^2/4a$ and $c = b/2a$. In the process of meshing, whereas several cycles of meshing are considered (Fig. 4(b)), the resulting function $\Delta\psi_2(\psi_1)$ of transmission errors becomes a symmetric parabolic function.

The authors have developed computerized synthesis of formate-cut spiral bevel gears that is based on simultaneous application of local synthesis and simulation of meshing and contact of gear tooth surfaces.

The purpose of local synthesis is to determine the pinion machine-tool settings considering as given: (i) the gear machine-tool settings, and (ii) the conditions of meshing and contact at the mean contact point M such as the tangent to the path of contact at M, the major axis of the contact ellipse at M, and the derivative of the function of transmission errors.

The purpose of simulation of meshing and contact is the determination of the bearing contact and function of transmission errors knowing the pinion and gear machine-tool settings.

The applied computational procedures are iterative processes with the goals to obtain: (i) a longitudinally directed bearing contact, (ii) a parabolic function of transmission errors with limited value of maximal errors, and (iii) reduced sensitivity of the gear drive to errors of alignment.

3. Derivation of Gear Tooth Surface [7, 9]

Applied Coordinate Systems: Coordinate system S_{m_2} is the fixed one and it is rigidly connected to the cutting machine (Fig. 5). Fig. 5(a) and 5(b) show two sets of coordinate systems applied for generations of left and right hand gears, respectively. Coordinate system S_2 is rigidly connected to the gear. Coordinate system S_g is rigidly connected to the gear head-cutter. It is considered that the gear head-cutter is a surface of revolution, and the rotation of the head cutter about the X_g – axis does not affect the process of generation.

The installment of the tool on the machine is determined by parameters H_2 and V_2, that are called horizontal and vertical settings. Parameters X_G and γ_{m_2} represent the settings of the gear.

Head Cutter Surface: The blades of the gear head-cutter of a parabolic profiles are shown in Fig. 6(a). Each side of the blade generates two sub-surfaces. The segment a of the parabolic profile generates the working part of the gear tooth surface. The circular arc of radius ρ_w generates the fillet of the gear tooth surface. The generating surfaces of the head-cutter are formed by rotation of the blade about the X_g – axis of the head-cutter (Figs. 6(b) and 6(c)); the rotation angle is θ_g. Therefore, the generating surfaces are: (i) surface of revolution formed by rotation of the blade of parabolic profile, and (ii) the surface of the torus formed by rotation of the circular arc profiles. A point on the generating surface is determined by parameters u_g and θ_g for the working surface, and by λ_w and θ_g for the fillet surface. Angle α_g is formed

between the tangent line of the blade at point M and the vertical center line of the blade. Parameter u_g measured from point M in the chosen direction is considered as a positive one, and angles α_g and λ_w as the acute ones. The apex of the parabola is located at point M determined by parameter s_{g_0}.

The surface of revolution and the torus surface of the head-cutter are designated as parts *(a)* and *(b)* of the head-cutter generating surface. Surface $\Sigma_g^{(a)}$ of the head-cutter is represented by vector function $\mathbf{r}_\mathbf{g}^{(\mathbf{a})}(u_g,\theta_g)$ as follows

$$\mathbf{r}_\mathbf{g}^{(\mathbf{a})}(u_g,\theta_g)=\begin{bmatrix} -u_g\cos\alpha_g+a_c u_g^2\sin\alpha_g-s_{g_0}\cos\alpha_g \\ (R_g\pm s_{g_0}\sin\alpha_g\pm u_g\sin\alpha_g\pm a_c u_g^2\cos\alpha_g)\sin\theta_g \\ (R_g\pm s_{g_0}\sin\alpha_g\pm u_g\sin\alpha_g\pm a_c u_g^2\cos\alpha_g)\cos\theta_g \end{bmatrix} \tag{3}$$

where u_g and θ_g are the surface coordinates, α_g is the blade angle at point M, R_g is the cutter point radius (Fig. 6) and given by

$$R_g=R_u\pm\frac{P_{w_2}}{2} \tag{4}$$

The upper and lower signs in equations (3) and (4) correspond to the concave and convex sides of the gear tooth, respectively.

The unit normal to the gear generating surface $\Sigma_g^{(a)}$ is represented by the equations

$$\mathbf{n}_\mathbf{g}^{(\mathbf{a})}(u_g,\theta_g)=\frac{\mathbf{N}_g^{(a)}}{\left|\mathbf{N}_g^{(a)}\right|},\quad \mathbf{N}_g^{(a)}=\frac{\partial\mathbf{r}_\mathbf{g}^{(\mathbf{a})}}{\partial u_g}\times\frac{\partial\mathbf{r}_\mathbf{g}^{(\mathbf{a})}}{\partial\theta_g} \tag{5}$$

Equations (3) and (5) yield

$$\mathbf{n}_\mathbf{g}^{(\mathbf{a})}(u_g,\theta_g)=\begin{bmatrix} \pm(\sin\alpha_g+2a_c u_g\cos\alpha_g) \\ (\cos\alpha_g-2a_c u_g\sin\alpha_g)\sin\theta_g \\ (\cos\alpha_g-2a_c u_g\sin\alpha_g)\cos\theta_g \end{bmatrix}\div\sqrt{1+4a_c^2u_g^2} \tag{6}$$

Surface $\Sigma_g^{(b)}$ is represented in S_g as

$$\mathbf{r}_\mathbf{g}^{(b)}(\lambda_w,\theta_g)=\begin{bmatrix} -\rho_w(1-\cos\lambda_w) \\ (X_g\pm\rho_w\sin\lambda_w)\sin\theta_g \\ (X_g\pm\rho_w\sin\lambda_w)\cos\theta_g \end{bmatrix} \tag{7}$$

where

$$X_g=R_g\mp\rho_w(1-\sin\alpha_g)/\cos\alpha_g$$

Here, ρ_w is the fillet radius of the gear generating surface.

The unit normal to the gear generating surface $\Sigma_g^{(b)}$ is represented by the equations

$$\mathbf{n}_\mathbf{g}^{(b)}(\lambda_w,\theta_g)=\frac{\mathbf{N}_g^{(b)}}{\left|\mathbf{N}_g^{(b)}\right|},\quad \mathbf{N}_g^{(b)}=\frac{\partial \mathbf{r}_\mathbf{g}^{(b)}}{\partial \lambda_w}\times\frac{\partial \mathbf{r}_\mathbf{g}^{(b)}}{\partial \theta_g} \tag{8}$$

Equations (8) yield

$$\mathbf{n}_\mathbf{g}^{(b)}(\lambda_w,\theta_g)=\begin{bmatrix}\pm\cos\lambda_w\\ \sin\lambda_w\sin\theta_g\\ \sin\lambda_w\cos\theta_g\end{bmatrix} \tag{9}$$

Equations of Head-Cutter Surfaces in S_2: Applying coordinate transformation from S_g to S_2, the gear tooth surfaces can be represented in S_2 by the equations

$$\mathbf{r}_2^{(a)}(u_g,\theta_g)=\mathbf{M}_{2\mathbf{g}}\mathbf{r}_\mathbf{g}^{(\mathbf{a})}(u_g,\theta_g) \tag{10}$$

$$\mathbf{r}_2^{(b)}(\lambda_w,\theta_g)=\mathbf{M}_{2\mathbf{g}}\mathbf{r}_\mathbf{g}^{(b)}(\lambda_w,\theta_g) \tag{11}$$

Here

$$\mathbf{M}_{2g}=\mathbf{M}_{2m_2}\mathbf{M}_{m_2g} \tag{12}$$

$$\mathbf{M}_{m_2g}=\begin{bmatrix}1&0&0&0\\0&1&0&\pm V_2\\0&0&1&H_2\\0&0&0&1\end{bmatrix}$$

$$\mathbf{M}_{2m_2}=\begin{bmatrix}\cos\gamma_{m_2}&0&-\sin\gamma_{m_2}&0\\0&1&0&0\\\sin\gamma_{m_2}&0&\cos\gamma_{m_2}&-X_G\\0&0&0&1\end{bmatrix}$$

Here,: V_2, H_2 and X_G are the gear machine tool settings. The upper and lower signs in front of V_2 correspond to right hand and left hand gears respectively. The whole set of gear machine tool settings is represented in Table 1. Remember that the generated gear tooth surface is a copy of the surface of the head-cutter, that is a surface of revolution. The rotation of the head-cutter about the X_g – axis that is necessary for the cutting or grinding process does not affect the shape of gear tooth surfaces.

The geometric model of gear tooth surfaces is shown in Fig. 7.

Table 1: Gear Machine Tool Settings

Blade angle α_g (Fig. 6)
Blade parabola coefficient α_c

Cutter radius R_u (mm) (Fig. 6)
Point width P_{w_2} (mm) (Fig. 6)
Cutter point radius R_g (mm) (Fig. 6)
Horizontal settings H_2 mm) (Fig. 5)
Vertical settings V_2 (Fig. 5)
Machine center to back X_G (mm) (Fig. 5)
Machine root angle γ_{m_2} (Fig. 5)
Fillet radius ρ_w (mm) (Fig. 6)

4. Derivation of Pinion Tooth Surface [7, 9, 10]

Applied Coordinate Systems: Coordinate systems applied for generation of pinion are shown in Fig. 8 and 9. Fig. 9(a) and (b) correspond to generation of right and left hand pinions, respectively. Coordinate systems S_{m_1}, S_{a_1} and S_{b_1} are the fixed ones and they are rigidly connected to the cutting machine. The movable coordinate systems S_1 and S_{c_1} are rigidly connected to the pinion and the cradle, respectively. They are rotated about the Z_{m_1} – axis and Z_{b_1} – axis, respectively, and their rotations are related with a polynomial function $\psi_1(\psi_{c_1})$, if modified roll is applied (see below). The ratio of instantaneous angular velocities of the pinion and the cradle is defined as $m_{1c}(\psi_1(\psi_{c_1}))=\omega^{(1)}(\psi_{c_1})/\omega^{(c)}$. The magnitude of $m_{1c}(\psi_1)$ at $\psi_{c1}=0$ is called ratio of roll. Parameters X_{D_1}, X_{B_1}, E_{m_1}, and γ_{m_1} are the basic machine tool settings for pinion generation.

Head Cutter Surfaces: The pinion generating surfaces are formed by surface $\Sigma_p^{(a)}$ and $\Sigma_p^{(b)}$ generated by straight-line and circular arc parts of the blades (Fig. 10). Surface $\Sigma_p^{(a)}$ is represented as

$$\mathbf{r}_p^{(a)}(s_p,\theta_p)=\begin{bmatrix}(R_p \mp s_p\sin\alpha_p)\cos\theta_p\\(R_p \mp s_p\sin\alpha_p)\sin\theta_p\\-s_p\cos\alpha_p\end{bmatrix} \tag{13}$$

where s_p and θ_p are the surface coordinates; α_p is the blade angle; R_p is the cutter point radius (Fig. 10). The upper and lower signs in equations (13) correspond to the convex and concave sides of the pinion tooth respectively.

The unit normal to the pinion generating surface $\Sigma_p^{(a)}$ is represented by the equations

$$\mathbf{n}_p^{(a)}(\theta_p)=\frac{\mathbf{N}_p^{(a)}}{\left|\mathbf{N}_p^{(a)}\right|},\quad \mathbf{N}_p^{(a)}=\frac{\partial\mathbf{r}_p^{(a)}}{\partial s_p}\times\frac{\partial\mathbf{r}_p^{(a)}}{\partial\theta_p} \tag{14}$$

Equations (13) and (14) yield

$$\mathbf{n}_p^{(a)}(\theta_p)=\begin{bmatrix}\cos\alpha_p\cos\theta_p\\\cos\alpha_p\sin\theta_p\\\mp\sin\alpha_p\end{bmatrix} \tag{15}$$

For the fillet surface $\Sigma_p^{(b)}$ we obtain

$$\mathbf{r}_p^{(b)}(\lambda_f,\theta_p)=\begin{bmatrix}(X_f \mp \rho_f \sin\lambda_f)\cos\theta_p\\(X_f \mp \rho_f \sin\lambda_f)\sin\theta_p\\-\rho_f(1-\cos\lambda_f)\end{bmatrix} \tag{16}$$

where

$$X_f = R_p \pm \rho_f(1 \mp \sin\alpha_p)/\cos\alpha_p$$

and ρ_f is the radius of the tool fillet.

The unit normal to the pinion generating surface $\Sigma_p^{(b)}$ is represented by the equations

$$\mathbf{n}_p^{(b)}(\lambda_f,\theta_p)=\frac{\mathbf{N}_p^{(b)}}{\left|\mathbf{N}_p^{(b)}\right|}, \quad \mathbf{N}_p^{(b)}=\frac{\partial \mathbf{r}_p^{(b)}}{\partial\lambda_f}\times\frac{\partial \mathbf{r}_p^{(b)}}{\partial\theta_p} \tag{17}$$

Equations (17) yield

$$\mathbf{n}_p^{(b)}(\lambda_f,\theta_p)=\begin{bmatrix}\sin\lambda_f\cos\theta_p\\\sin\lambda_f\sin\theta_p\\\mp\cos\lambda_f\end{bmatrix} \tag{18}$$

The head-cutter is mounted on coordinate system S_{c_1} called the cradle of the cutting machine and its installment is determined by settings S_{r_1} and q_1 (Fig. 9). In the process of pinion generation coordinate systems S_{c_1} and S_1 performed related rotations with respect to S_{m_1}. Then, in coordinate system S_1, a family of pinion head-cutter surfaces is generated and determined as:

$$\mathbf{r}_1^{(a)}(s_p,\theta_p,\psi_1)=\mathbf{M}_{1p}(\psi_1)\mathbf{r}_p^{(a)}(s_p,\theta_p) \tag{19}$$

$$\mathbf{r}_1^{(b)}(\lambda_f,\theta_p,\psi_1)=\mathbf{M}_{1p}(\psi_1)\mathbf{r}_p^{(b)}(\lambda_f,\theta_p) \tag{20}$$

where ψ_1 is the generalized parameter of motion, and

$$\mathbf{M}_{1p}=\mathbf{M}_{1b_1}\mathbf{M}_{b_1a_1}\mathbf{M}_{a_1m_1}\mathbf{M}_{m_1c_1}\mathbf{M}_{c_1p}$$

$$\mathbf{M}_{c_1p}=\begin{bmatrix}1&0&0&S_{r_1}\cos q_1\\0&1&0&\pm S_{r_1}\sin q_1\\0&0&1&0\\0&0&0&1\end{bmatrix}$$

$$\mathbf{M}_{m_1c_1}=\begin{bmatrix}\cos\psi_{c_1} & -\sin\psi_{c_1} & 0 & 0\\ \sin\psi_{c_1} & \cos\psi_{c_1} & 0 & 0\\ 0 & 0 & 1 & 0\\ 0 & 0 & 0 & 1\end{bmatrix}$$

$$\mathbf{M}_{a_1m_1}=\begin{bmatrix}1 & 0 & 0 & 0\\ 0 & 1 & 0 & E_{m_1}\\ 0 & 0 & 1 & -X_{B_1}\\ 0 & 0 & 0 & 1\end{bmatrix}$$

$$\mathbf{M}_{b_1a_1}=\begin{bmatrix}\sin\gamma_{m_1} & 0 & -\cos\gamma_{m_1} & 0\\ 0 & 1 & 0 & 0\\ \cos\gamma_{m_1} & 0 & \sin\gamma_{m_1} & -X_{D_1}\\ 0 & 0 & 0 & 1\end{bmatrix}$$

$$\mathbf{M}_{1b_1}=\begin{bmatrix}\cos\psi_1 & \sin\psi_1 & 0 & 0\\ -\sin\psi_1 & \cos\psi_1 & 0 & 0\\ 0 & 0 & 1 & 0\\ 0 & 0 & 0 & 1\end{bmatrix}$$

The upper and lower signs of $S_{r_1}\sin q_1$ in matrix $\mathbf{M}_{c_1p}$ correspond to generation of right and left hand pinions, respectively. Where the modified roll is applied in the process of generation, the rotation angles ψ_1 and ψ_{c_1} of the pinion and cradle are related as

$$\psi_1=m_{1c}\psi_{c_1}+b_2\psi_{c_1}^2+b_3\psi_{c_1}^3 \tag{21}$$

where b_2 and b_3 are the modified roll coefficients.

The derivative of function $\psi_1(\psi_{c_1})$ taken at $\psi_{c_1}=0$ determines the so-called ratio of roll represented in equation (21) by m_{1c}.

Equation of Meshing: The pinion tooth surface Σ_1 is the envelope to the family of head-cutter surfaces. Surface Σ_1 consists of two surfaces $\Sigma_1^{(a)}$ and $\Sigma_1^{(b)}$ which correspond to the cutter surfaces $\Sigma_p^{(a)}$ and $\Sigma_p^{(b)}$, respectively. Modified roll is applied in the process of generation. For generation of surface $\Sigma_1^{(a)}$, the equation of meshing is represented as

$$\mathbf{n}_{m_1}^{(a)}\cdot\mathbf{v}_{m_1}^{(p1)}=f_{1p}^{(a)}(s_p,\theta_p,\psi_1)=0 \tag{22}$$

where $\mathbf{n}_{m_1}^{(a)}$ the unit normal to the surface, and $\mathbf{v}_{m_1}^{(p1)}$ is the velocity in relative motion. These vectors are represented in the fixed coordinate system S_{m_1} as follows:

$$\mathbf{n}_{m_1}^{(a)}=\mathbf{L}_{m_1c_1}\mathbf{L}_{c_1p}\mathbf{n}_p^{(a)}(\theta_p) \tag{23}$$

$$\mathbf{v}_{m_1}^{(p1)} = [(\boldsymbol{\omega}_{m_1}^{(p)} - \boldsymbol{\omega}_{m_1}^{(1)}) \times \mathbf{r}_{m_1} - (\overline{\mathbf{O}_{m_1}\mathbf{O}_{a_1}} \times \boldsymbol{\omega}_{m_1}^{(1)}) \tag{24}$$

Here

$$\mathbf{r}_{m_1} = \mathbf{M}_{m_1 c_1} \mathbf{M}_{c_1 p} \mathbf{r}_p^{(a)}(s_p, \theta_p)$$

$$\overline{\mathbf{O}_{m_1}\mathbf{O}_{a_1}} = [0, \quad -E_{m_1}, \quad X_{B_1}]^T$$

$$\boldsymbol{\omega}_{m_1}^{(1)} = [\cos\gamma_{m_1}, \quad 0, \quad \sin\gamma_{m_1}]^T$$

$$\boldsymbol{\omega}_{m_1}^{(p)} = [0, \quad 0, \quad m_{c1}(\psi_1)]^T$$

The ratio m_{c1} is not constant since modified roll is applied and can be represented as

$$m_{c1} = \frac{\omega_{c_1}}{\omega_1} = \frac{d\psi_{c_1}}{dt} \Big/ \frac{d\psi_1}{dt} = \frac{1}{m_{1c} + 2b_2\psi_1 + 3b_3\psi_1^2} \tag{25}$$

where b_2 and b_3 are modified roll coefficients.

Finally, we obtained the equations for pinion tooth surface part (a) as

$$\mathbf{r}_1^{(a)}(s_p, \theta_p, \psi_1) = \mathbf{M}_{1p}(\psi_1)\mathbf{r}_p^{(a)}(s_p, \theta_p) \tag{26}$$

$$f_{1p}^{(a)}(s_p, \theta_p, \psi_1) = 0 \tag{27}$$

Similarly, the fillet surface of pinion tooth surface $\Sigma_1^{(b)}$ may be represented as

$$\mathbf{r}_1^{(b)}(\lambda_f, \theta_p, \psi_1) = \mathbf{M}_{1p}(\psi_1)\mathbf{r}_p^{(b)}(\lambda_f, \theta_p) \tag{28}$$

$$f_{1p}^{(b)}(\lambda_f, \theta_p, \psi_1) = 0 \tag{29}$$

The geometric model of pinion tooth surfaces is shown in Fig. 11.

5. Procedures of Proposed Design

The authors have developed an approach for the design of formate cut spiral bevel gears that provides a stabilized bearing contact and reduced level of noise. The bearing contact is of a longitudinal direction that enables to increase the contact ratio, avoid edge contact and reduce the shift of the bearing contact caused by misalignment. The reduction of noise is achieved by application of a predesigned parabolic function of transmission errors and limitation of maximal transmission errors caused by misalignment. The approach is based on three procedures that require simultaneous execution of computer programs developed for the local synthesis and simulation of meshing and contact of the gear drive.

The purpose of the local synthesis is to determine the pinion machine-tool settings for the following conditions of meshing and contact of pinion-gear tooth surfaces Σ_1 and Σ_2:

(i) The gear machine-tool settings are considered as given (they may be adapted, for instance, from a Gleason summary for gear generation);

(ii) The pinion-gear tooth surfaces Σ_1 and Σ_2 are in tangency at a chosen mean contact point M (Fig. 12);

(iii) Parameters $2a$, η_2, and $m_{12}^{'}$ are assigned ahead and determine the conditions of meshing and contact of Σ_1 and Σ_2 at point M and in the neighborhood of M. Here, $2a$ is the major axis of the instantaneous contact ellipse, η_2 determines the tangent to the path of contact on the gear tooth surface at M, and $m_{12}^{'}$ is the derivative $\frac{\partial}{\partial \phi_1}(m_{12}^{'}(\phi_1))$ at point M, where $m_{12}(\phi_1)$ is the gear ratio.

Note: It will be shown in section 6 that the location of point M_2 on the gear tooth surface as the candidate for the mean contact point of Σ_1 and Σ_2 may be chosen. Then, the procedure of the local synthesis permits the determination of point M_1 on pinion tooth surface Σ_1 that will be in tangency with Σ_2 at the chosen point M_2 of Σ_2.

The simulation of meshing and contact of pinion-gear tooth surfaces is accomplished by application of the TCA (Tooth Contact Analysis) computer program developed. The input for TCA are the equations of pinion-gear tooth surfaces, parameters of motion and assembly. The output is the bearing contact and the function of transmission errors.

The design is based on simultaneous execution of computer programs developed for local synthesis and TCA, it is an iterative process and requires application of following three procedures.

Procedure 1:

The path of contact on gear tooth surface is a spatial curve L. Projection of L on tangent plane T (Fig. 13) is designated by L_T. The purpose of procedure 1 is to obtain that L_T is a straight line directed longitudinally. Fig. 13 shows projections $L_T^{(1)}$ and $L_T^{(2)}$ that deviate from the desired line L_T.

Fig. 14 shows the flow chart that describes the steps of procedure 1. The procedure of computation is an iterative process and requires variation of parameter $m_{12}^{'}$. The steps of the procedure are as follows:

Step 1: Input the gear machine-tool settings into the program of local synthesis.
Step 2: Input parameters $2a$, η_2, and $m_{12}^{'}$ into the program of local synthesis.
Step 3: Execute the program of local synthesis.
Step 4: Determine from the program of local synthesis the pinion machine-tool settings.
Step 5: Using the machine-tool settings obtained, compute the pinion and gear tooth surfaces Σ_1 and Σ_2.
Step 6: Execute TCA computer program and obtain projection L_T of path of contact L on tangent plane T (Fig. 13).
Step 7: Execute the iterative process and obtain projection of path of contact L_T as a straight line by variation of $m_{12}^{'}$.
Step 8: Output the final machine-tool settings for the pinion.

The iterative process is based on the following considerations:
(1) The TCA computer program applied determines projection L_T of path of contact numerically.
(2) Consider L_T in coordinate system S_t (Fig. 13) which origin coincides with M and axes (x_t, y_t) are located in plane T. Axis x_t is the tangent to L_T at point M.

(3) Represent projection L_T as a parabolic regression equation by using a subroutine of regression [11]

$$y_t(x_t, m_{12}') = \beta_0(m_{12}') + \beta_1(m_{12}')x_t + \beta_2(m_{12}')x_t^2 \tag{30}$$

where m_{12}' is the input parameter that is varied in the process of iteration

(4) The goal is to represent L_T as a straight line that might be obtained by such a magnitude of m_{12}' whereas coefficient $\beta_2(m_{12}') = 0$ (see equation (30)). The iterations for determination of $\beta_2(m_{12}') = 0$ are executed by applying the secant method [12] and illustrated by Fig. 15. Equation (30) with $\beta_2(m_{12}') = 0$ provides the projection of path of contact as a straight line.

Procedure 2:

Procedure 1 discussed above provides the desired longitudinal path of contact and bearing contact. However, the shape of the obtained function of transmission errors and the magnitude of maximal transmission errors do not satisfy the requirements of low-noise gear drive. The goal of procedure 2 is to obtain a parabolic function of negative transmission errors and of limited value of maximal errors.

The sequence of steps applied for procedure 2 is represented by the flow chart shown in Fig. 16.

At the start, we use the pinion and gear machine tool settings obtained in procedure 1, but consider that the pinion is generated by application of modified roll. Then, we compute the gear and pinion tooth surfaces Σ_1 and Σ_2, and use them for the TCA computer program. The intermediate output of TCA is a function of transmission errors. We compare it with the sought-for parabolic function of transmission errors and determine the necessary corrections using modified roll. Repeating the procedure discussed above, we can obtain the sought-for parabolic function of transmission errors.

Analytically, the algorithm of procedure 2 is represented as follows.

Step 1: Function of transmission errors $\Delta\phi_2(\phi_1)$ obtained from TCA is numerically represented as a polynomial function up to third order to be included [11]

$$\Delta\phi_2^{(1)}(\phi_1) = a_0 + a_1\phi_1 + a_2\phi_1^2 + a_3\phi_1^3 \tag{31}$$

The shape and magnitude of maximal errors of function $\Delta\phi_2^{(1)}(\phi_1)$ do not satisfy the requirements of a low-noise gear drive. Function (31) has to be transformed into a parabolic function with limited magnitude of transmission errors by application of procedure 2.

Step 2: We apply for transformation of function $\Delta\phi_2^{(1)}(\phi_1)$ the modified roll for generation of the pinion that is represented as

$$\psi_1(\psi_{c_1}) = m_{1c}\psi_{c_1} + b_2\psi_{c_1}^2 + b_3\psi_{c_1}^3 \tag{32}$$

Here, ψ_1 and ψ_2 are the angles of rotation of the pinion and the cradle performed during the process for generation, m_{1c} is the first derivative of $\psi_1(\psi_{c_1})$ taken at $\psi_{c_1} = 0$ and obtained by the procedure of local

synthesis (see section 6). Coefficients b_2 and b_3 have to be determined by using an iterative process (see below).

Step 3: Assigning coefficients b_2 and b_3 of modified roll and using pinion machine-tool settings obtained in procedure 1, we may determine the pinion tooth surface Σ_1. The gear tooth surface Σ_2 is considered as given.

Step 4: Applying TCA for simulation of meshing of Σ_1 and Σ_2 we may obtain numerically the modified function of transmission errors and then represent it again by polynomial function (31) with new magnitudes of coefficients a_0, a_1, a_2 and a_3.

Procedure 2 with steps 1 to 4 has to be repeated until a parabolic function of transmission errors $\Delta\phi_2(\phi_1)$ with limited magnitude of maximal transmission errors is obtained.

The computation is an iterative process based on application of secant method of numerical computations [12]. The goal is to transform the shape of obtained function $\Delta\phi_2^{(1)}(\phi_1)$ of transmission errors into a parabolic function

$$\Delta\phi_2(\phi_1) = -a_2\phi_1^2 \ , \ -\frac{\pi}{N_1} \le \phi_1 \le \frac{\pi}{N_1} \tag{33}$$

where

$$\left|\Delta\phi_2(\phi_1)\right|_{\max} = a_2\left(\frac{\pi}{N_1}\right)^2 = \Delta\Phi \tag{34}$$

This goal is accomplished by variation of coefficients b_2 and b_3 of function (32) provided by modified roll. The variation of b_2 and b_3 is performed independently and is illustrated by drawings of Fig. 17.

Fig. 17(a) illustrates variation of coefficient b_3 of modified roll for obtaining of coefficient $a_3 = 0$ of function (31). Function $a_2(b_2)$ is determined as the output of TCA by variation of modified roll.

Fig. 17(b) illustrates variation of coefficient b_2 of modified roll for obtaining of $\left|\Delta\phi_2(\phi_1)\right|_{\max} = \Delta\Phi$.

Function $\Delta\phi_2(\phi_1)$ is determined as the output of TCA by variation of b_2.

Procedure 3:

Procedures 1 and 2 are performed by simultaneous application of computer programs of local synthesis and TCA, but the errors of alignment of the gear drive are not considered.

The purpose of procedure 3 is to adjust the gear drive for the existence of errors of alignment. This is achieved by adjusting the previously designed path of contact to the assigned or expected errors of alignment. The procedure is based on the flow chart shown in Fig. 18.

The adjustment of the gear drive to the errors of alignment is performed by correction of parameter η_2 (Fig. 12) that determines the orientation of the path of contact on the gear tooth surface.

The prescribed procedure yields that in some cases of design it becomes necessary to deviate the path of contact from the longitudinal direction to reduce the shift of bearing contact by errors of alignment. The procedure has to be applied for separate simulation of each error of alignment for obtaining the required correction of η_2. The permissible tolerance of each alignment error is obtained by procedure 3.

Local Synthesis and Determination of Pinion Machine Tool Settings [7, 8, 9]

Remembering that the local synthesis is accomplished simultaneously with the TCA, and the computation is an iterative process. The computer program developed permits the determination at each iteration the pinion machine-tool settings.

The input parameters for the local synthesis are the gear machine-tool settings and parameters η_2 , a and $m_{12}^{'}$ (see Flow chart, Fig. 14).

The procedure of the local synthesis is as follows.

Stage 1: Determination of the mean contact point on the gear tooth surface

Step 1: Mean point A on surface Σ_2 is chosen by designation of parameters L_A and R_A (Fig. 19), where A is the candidate for the mean contact point M of surfaces Σ_2 and Σ_1. Then we obtain the following system of two equations in two unknowns

$$\left.\begin{aligned} Z_2(u_g^*,\theta_g^*) &= L_A \\ X_2^2(u_g^*,\theta_g^*)+Y_2^2(u_g^*,\theta_g^*) &= R_A^2 \end{aligned}\right\} \tag{35}$$

where X_2, Y_2 and Z_2 are the projections of position vector $\mathbf{r}_2(u_g^*,\theta_g^*)$.

Step 2: Equations (35) considered simultaneously permits the surface parameters (u_g^*,θ_g^*) to be determined for point A. Vector functions $\mathbf{r}_g(u_g,\theta_g)$ and $\mathbf{n}_g(\theta_g)$ determine the position vector and surface unit normal for a current point of gear tooth surface Σ_g. Taking in these vector functions $u_g = u_g^*$ and $\theta_g = \theta_g^*$, we can determine the position vector $\mathbf{r}_g^{(A)}$ of point A and the surface unit normal $\mathbf{n}_g^{(A)}$ at A.

Step 3: Parameters u_g^* and θ_g^* and the unit vectors $\mathbf{e}_g$ and $\mathbf{e}_u$ of principal directions on surface Σ_g are considered as known. Here:

$$\mathbf{e}_g = \frac{\partial \mathbf{r}_g^{(a)}}{\partial u_g} \div \left|\frac{\partial \mathbf{r}_g^{(a)}}{\partial u_g}\right| = \begin{bmatrix} -\cos\alpha_g + 2a_c u_g \sin\alpha_g \\ (\pm\sin\alpha_g \pm 2a_c u_g \cos\alpha_g)\sin\theta_g \\ (\pm\sin\alpha_g \pm 2a_c u_g \cos\alpha_g)\cos\theta_g \end{bmatrix} \div \sqrt{1+4a_c^2 u_g^2} \tag{36}$$

$$\mathbf{e}_u = \frac{\partial \mathbf{r}_g^{(a)}}{\partial \theta_g} \div \left| \frac{\partial \mathbf{r}_g^{(a)}}{\partial \theta_g} \right| = \begin{bmatrix} 0 \\ \cos\theta_g \\ -\sin\theta_g \end{bmatrix} \tag{37}$$

The gear generating surface is a surface of revolution, and the principal curvatures k_g and k_u of Σ_g are determined by the following equations:

$$\begin{cases} k_g = \dfrac{2a_c}{(1+4a_c^2 u_g^2)^{\frac{3}{2}}} \\ k_u = \dfrac{-\cos\alpha_g + 2a_c u_g \sin\alpha_g}{(R_g \pm s_{g_0}\sin\alpha_g \pm u_g \sin\alpha_g \pm a_c u_g^2 \cos\alpha_g)\sqrt{1+4a_c^2 u_g^2}} \end{cases} \tag{38}$$

The upper and lower signs correspond to the concave and convex sides of gear tooth, respectively.

The unit vectors $\mathbf{e}_s$ and $\mathbf{e}_q$ of principal directions on surface Σ_2 are obtained by using matrix transformation from S_g to S_2. The gear principal curvatures k_s and k_q of Σ_2 are the same as the principal curvatures k_g and k_u, respectively, of the gear head-cutter.

Stage 2: Tangency of Surfaces Σ_2 (Σ_g) and Σ_1 at Mean Contact Point *M*.

Step 1: The derivations accomplished at stage 1 permits the position vector $\mathbf{r}_2^{(A)}$ to be determined and the surface unit normal $\mathbf{n}_2^{(A)}$ of point *A* of tangency of surfaces Σ_2 (Σ_g). The goal now is to determine such a point *M* in the fixed coordinate system S_l (Fig. 20) where two surfaces Σ_2 (Σ_g) and Σ_1 are in tangency with each other.

Surfaces Σ_2 and Σ_g are the same ones, because there is no relative motion between the cradle and workpiece (between coordinate system S_2 to S_g whereas the gear is generated. Using coordinate transformation from S_2 to S_l (Fig. 20), we may obtain $\mathbf{r}_l^{(A)}$ and $\mathbf{n}_l^{(A)}$. The new position of point *A* in S_l will become point *M* of tangency of Σ_2 and Σ_1, if the following equation of meshing between Σ_2 and Σ_1 is observed

$$\mathbf{n}_l^{(A)}(\phi_2^{(0)}) \cdot \mathbf{v}_l^{(21,A)}(\phi_2^{(0)}) = 0 \tag{39}$$

Here, $\mathbf{n}_l^{(A)} \equiv \mathbf{n}_l^{(M)}$ and $\mathbf{v}_l^{(12,A)} \equiv \mathbf{v}_l^{(12,M)}$; $\mathbf{v}_l^{(12,A)}$ is the relative velocity at point *A* determined with the ideal gear ratio

$$m_{21}^{(0)} = \frac{\omega^{(2)}}{\omega^{(1)}} \tag{40}$$

The solution of equation (39) for $\phi_2^{(0)}$ provides the value of the initial turning angle for ϕ_2. It is evident that two surfaces Σ_2 and Σ_1 are now in tangency with each other at point *M*.

Step 2: We consider as known at point M the principal curvatures k_s and k_q of surface Σ_2, and the unit vectors $\mathbf{e}_s$ and $\mathbf{e}_q$ of principal directions on Σ_2. The unit vectors $\mathbf{e}_s$ and $\mathbf{e}_q$ are represented in S_l. The goal now is to determine at point M the principal curvatures and k_f and k_h of surface Σ_1, and the unit vectors $\mathbf{e}_f$ and $\mathbf{e}_h$ of principal directions on Σ_1. This goal can be achieved by application of the procedure described in Appendix 1. It is shown in Appendix 1 that the determination of k_f, k_h, $\mathbf{e}_f$ and $\mathbf{e}_h$ becomes possible if parameters m_{21}, η_2 (or η_1), and a/δ are assumed to be known or are used as input data.

Stage 3: Tangency of Surfaces $\Sigma_2(\Sigma_g)$, Σ_1 and Σ_p at Mean Contact Point M.

Basic Equations: Tangency of $\Sigma_2(\Sigma_g)$ and Σ_1 at mean contact point M has been already provided at the previous stages. The position vector $\mathbf{r}_l^{(M)}$ of point M and the surface unit normal $\mathbf{n}_l^{(M)}$ at point M were determined in coordinate system S_l. Let us imagine now that coordinate system S_1 that coincides with S_l and surface Σ_1 are installed in coordinate system S_{m_1} (Fig. 8). Let angle $\psi_1^{(0)}$ be the installment angle of the pinion (it is the initial value of ψ_1). Using coordinate transformation from S_1 to S_{m_1}, we may determine in S_{m_1} position vector $\mathbf{r}_{m_1}^{(M)}$ of point M and the surface unit normal $\mathbf{n}_{m_1}^{(M)}$. In Appendix 1 the conditions of improved meshing and contact of pinion and gear tooth surfaces Σ_1 and Σ_2 are considered and then the relationships between the principal curvatures and directions of surfaces for such conditions of meshing and contact are determined (see equations (93)). The point of tangency of surfaces Σ_1 and Σ_p is designated in Appendix 1 as point B. The pinion generating surface Σ_p is installed in S_{m_1} taking the cradle angle ψ_{c_1} equal to zero. The position vector of point B of surface Σ_p and the surface unit normal at B are represented in S_{m_1} as $\mathbf{r}_{m_1}^{(B)}$ and $\mathbf{n}_{m_1}^{(B)}$. The tangency of Σ_1 and Σ_p at the mean contact point M is satisfied, if the following vector equations are observed

$$\mathbf{n}_{m_1}^{(M)} = \mathbf{n}_{m_1}^{(B)} \tag{41}$$

$$\mathbf{r}_{m_1}^{(M)} = \mathbf{r}_{m_1}^{(B)} \tag{42}$$

$$\mathbf{n}_{m_1}^{(M)} \cdot \mathbf{v}_{m_1}^{(1p)} = 0 \tag{43}$$

where equation (43) is the equation of meshing. Observation of equations (41)-(43) means that all of the three surfaces ($\Sigma_2(\Sigma_g)$, Σ_1 and Σ_p) are in contact at point M.

Using equations (41)-(43) and (93) from Appendix 1, it becomes possible to obtain the settings of the pinion and the head-cutter that guarantee the improved conditions of meshing and contact at point M. The machine tool settings to be determined are as follows:

(i) X_B, E_{m_1}, X_{D_1} and $m_{1p} = \omega^{(1)}/\omega^{(p)}$. Settings X_{B_1} and X_{D_1} are related by the following equation (Fig. 21)

$$X_{B_1} = -(X_{D_1} - |\overline{O_R O_1}|)\sin\gamma_{m_1} \tag{44}$$

where

$$\overline{|O_R O_1|} = \frac{[(A_m + F_w/2)\sin\gamma_1 - a_{d_1}\cos\gamma_1]}{\tan\gamma_{m_1}} - [(A_m + F_w/2)\cos\gamma_1 - a_{d_1}\sin\gamma_1]$$

Equation (44) is derived for the case of design of a spiral bevel gear with different apexes of the pitch and root cones.

(ii) Design parameter R_p of the head-cutter (Fig. 10).

(iii) Parameters S_{r_1} and q_1 that determine the installment of the head-cutter on the cradle (Fig. 9).

(iv) Parameter $\psi_1^{(0)}$ is the initial angle ψ_1 for installment of coordinate system S_1 with respect to S_{b_1} (Fig. 8), and parameter θ_p of the head-cutter surface Σ_p.

Computation of Pinion Machine-Tool Settings. The procedure for computation is as follows:

Step 1: Determine the values of θ_p and $\psi_1^{(0)}$ that are the sought-for two unknowns. Equation (41) is used for determination of θ_p and $\psi_1^{(0)}$, taking into account that

$$\mathbf{n}_{m_1}^{(M)}(\theta_p) = \begin{bmatrix} \cos\alpha_p \cos\theta_p \\ \cos\alpha_p \sin\theta_p \\ \mp\sin\alpha_p \end{bmatrix} \tag{45}$$

and

$$\mathbf{n}_{m_1}^{(M)} = \mathbf{L}_{m_1 b_1}\mathbf{L}_{b_1 1}\mathbf{n}_1^{(M)} \tag{46}$$

where $\mathbf{n}_1^{(M)} \equiv \mathbf{n}_l^{(M)}$ since S_1 coincides with S_l (Fig. 20). Here,

$$\mathbf{L}_{m_1 b_1} = \begin{bmatrix} \sin\gamma_{m_1} & 0 & \cos\gamma_{m_1} \\ 0 & 1 & 0 \\ -\cos\gamma_{m_1} & 0 & \sin\gamma_{m_1} \end{bmatrix} \tag{47}$$

$$\mathbf{L}_{b_1 1} = \begin{bmatrix} \cos\psi_1^{(0)} & -\sin\psi_1^{(0)} & 0 \\ \sin\psi_1^{(0)} & \cos\psi_1^{(0)} & 0 \\ 0 & 0 & 1 \end{bmatrix} \tag{48}$$

Equations (41) and (45)-(48) yield the following expressions for determination of θ_p and $\psi_1^{(0)}$

$$\cos\theta_p = \frac{n_{lz} \pm \sin\gamma_{m_1}\sin\alpha_p}{\cos\gamma_{m_1}\cos\alpha_p} \tag{49}$$

$$\sin\psi_1^{(0)} = \frac{-n_{ly}\cos\theta_p\cos\alpha_p + n_{lx}\sin\gamma_{m_1}\sin\theta_p\cos\alpha_p + n_{ly}n_{lz}\cos\gamma_{m_1}}{(n_{lx}^2 + n_{ly}^2)\sin\gamma_{m_1}} \tag{50}$$

$$\cos\psi_1^{(0)} = \frac{\sin\theta_p \cos\alpha_p - n_{lx}\sin\psi_1^{(0)}}{n_{ly}} \tag{51}$$

where α_p is the given value of the profile angle of the head-cutter, and n_{lx}, n_{ly} and n_{lz} are the three components of vector $\mathbf{n}_l^{(M)}$. The great advantage of the approach developed is that the requirement of the coincidence of the normals does not require a non-standard profile angle α_p or the tilt of the head-cutter with respect to the cradle.

Using θ_p, it becomes possible to determine the unit vectors $\mathbf{e}_p$ and $\mathbf{e}_t$ of principal directions on surface Σ_p at point *M*.

Step 2: Determination of pinion machine-tool settings X_{B_1} (X_{D_1}), E_{m_1}, m_{1p} and the design parameter R_p of the head-cutter (five unknowns are sought-for).

As a reminder, X_{B_1} and X_{D_1} are related by equation (44). The determination of the machine-tool settings mentioned above is based on application of the system of equations (93) and equation (43) that represent a system of four non-linear equations with four unknowns: X_{D_1}, E_{m_1}, m_{1p} and R_p.

The design parameters mentioned above provide as well improved conditions of meshing and contact at the mean contact point *M*.

Step 3: Determination of machine-tool settings S_{r_1} and q_1 and the pinion surface parameter s_p (three unknowns are sought-for).

Determination of the mentioned three parameters is based on application of equation (42), considering that generating surface Σ_p is a cone. The final equations for a right hand pinion are as follows:

$$S_{r_1}\cos q_1 + (R_p \mp s_p \sin\alpha_p)\cos\theta_p = X_{m1}^{(M)} \tag{52}$$

$$S_{r_1}\sin(\pm q_1) + (R_p \mp s_p \sin\alpha_p)\sin\theta_p = Y_{m1}^{(M)} \tag{53}$$

$$-s_p\cos\alpha_p = Z_{m1}^{(M)} \tag{54}$$

The upper and lower signs in front of q_1 in equation (53) correspond to the design of right-hand and left hand pinions, respectively.

The stages of computation discussed above may be summarized as follows:

(i) It is necessary to determine ten unknowns: six machine-tool settings (X_{B_1}, E_{m_1}, X_{D_1}, q_1, S_{r_1}, m_{1p}), two surface parameters (θ_p, s_p), one cutter parameter R_p and one position parameter $\psi_1^{(0)}$ which defines the pinion initial turn angle.

(ii) The equation system for determination of the unknowns is formed as follows:

$$\mathbf{n}_{m_1}^{(M)} = \mathbf{n}_{m_1}^{(B)} \tag{55}$$

$$\mathbf{r}_{m_1}^{(M)} = \mathbf{r}_{m_1}^{(B)} \tag{56}$$

$$\mathbf{n}_{m_1}^{(M)} \cdot \mathbf{v}_{\mathbf{m}_1}^{(1p)} = 0 \tag{57}$$

$$X_{B_1} = -(X_{D_1} - |\overline{O_R O_1}|)\sin\gamma_{m_1} \tag{58}$$

In addition, we use three curvature equations

$$\left.\begin{aligned} \tan 2\sigma^{(1p)} &= \frac{-2d_{13}d_{23}}{d_{23}^2 - d_{13}^2 - (k_f - k_h)d_{33}} \\ k_t - k_p &= \frac{-2d_{13}d_{23}}{d_{33}\sin 2\sigma^{(1p)}} \\ k_t + k_p &= k_f + k_h + \frac{d_{13}^2 + d_{23}^2}{d_{33}} \end{aligned}\right\} \tag{59}$$

Equation (55) is equivalent to two independent scalar equations, equations (56) is equivalent to three scalar equations, equations (57), (58) and (59) represent five scalar equations. Thus, the system of equations provides indeed ten scalar equations for determination of ten unknowns. The solution for the unknowns requires solution of a subsystem of four nonlinear equations (see step 2) and solution of six remaining equations represented in echelon form (each of the six equations contains one unknown to be determined).

7. Simulation of Meshing and Contact Accomplished in Procedure 1 (Section 5) [7, 8, 9]

The main goal of simulation of meshing and contact in procedure 1 (see Flow chart of Fig. 14) is to determine bearing contact that corresponds to pinion machine-tool settings obtained in section 6. Remembering that the computational procedures represented in sections 6 and 7 must be applied simultaneously, to represent an iterative process for determination of longitudinal path of contact. The developed TCA (Tooth Contact Analysis) computer program (based on simulation of meshing and contact) provides at each stage of iteration the path of contact. In addition, TCA provides the function of transmission errors which shape has to be corrected by application of pinion modified roll (see procedure 2 of section 5).

Applied Coordinate Systems: The meshing of gear tooth surfaces is considered in the fixed coordinate system S_h that is rigidly connected to the housing (Fig. 22). Movable coordinate system S_1 and S_2 are rigidly connected to the pinion and the gear, respectively. Auxiliary coordinate systems S_{b_1} and S_{b_2} are used to represent the rotation of the pinion (with respect to S_{b_1}) and the gear (with respect to S_{b_2}). The errors of alignment are simulated by respective installment of S_{b_1} and S_{b_2} with respect to S_h.

The errors of installment are: ΔH – the axial displacement of the pinion; $\Delta\gamma$ – the change of the shaft angle γ; ΔE – the shortest distance between the axes of the pinion and the gear when the pinion-gear axes are crossed instead of intersected; ΔD – the axial displacement of the gear. In the case of an aligned gear drive we consider that ΔH, $\Delta\gamma$, ΔE and ΔD are all equal to zero.

Simulation Algorithm: During the process of meshing, the pinion and gear tooth surfaces must be in continuous tangency and this can be provided, if at any instant their position vectors coincide and the surface normals are collinear. Instead of collinearity of surface normals, equality of surface unit normals may be required.

Pinion and gear tooth surfaces are represented in coordinate system S_h by the following equations

$$\mathbf{r}_h^{(1)}(s_p,\theta_p,\psi_1,\phi_1)=\mathbf{M}_{hb_1}\mathbf{M}_{b_1 1}(\phi_1)\mathbf{r}_1(s_p,\theta_p,\psi_1) \tag{60}$$

$$\mathbf{r}_h^{(2)}(u_g,\theta_g,\phi_2)=\mathbf{M}_{hb_2}\mathbf{M}_{b_2 2}(\phi_2)\mathbf{r}_2(u_g,\theta_g) \tag{61}$$

Here:

$$\mathbf{M}_{b_1 1}=\begin{bmatrix}\cos\phi_1 & \sin\phi_1 & 0 & 0\\ -\sin\phi_1 & \cos\phi_1 & 0 & 0\\ 0 & 0 & 1 & 0\\ 0 & 0 & 0 & 1\end{bmatrix}$$

$$\mathbf{M}_{hb_1}=\begin{bmatrix}1 & 0 & 0 & 0\\ 0 & 1 & 0 & 0\\ 0 & 0 & 1 & \Delta H\\ 0 & 0 & 0 & 1\end{bmatrix}$$

$$\mathbf{M}_{b_1 2}=\begin{bmatrix}\cos\phi_2 & -\sin\phi_2 & 0 & 0\\ \sin\phi_2 & \cos\phi_2 & 0 & 0\\ 0 & 0 & 1 & 0\\ 0 & 0 & 0 & 1\end{bmatrix}$$

$$\mathbf{M}_{hb_2}=\begin{bmatrix}\cos(\gamma+\Delta\gamma) & 0 & -\sin(\gamma+\Delta\gamma) & -\Delta D\sin(\gamma+\Delta\gamma)\\ 0 & 1 & 0 & \Delta E\\ \sin(\gamma+\Delta\gamma) & 0 & \cos(\gamma+\Delta\gamma) & \Delta D\cos(\gamma+\Delta\gamma)\\ 0 & 0 & 0 & 1\end{bmatrix}$$

Unit normals to surfaces of pinion and gear are represented in S_h by the following equations, respectively

$$\mathbf{n}_h^{(1)}(s_p,\theta_p,\psi_1,\phi_1)=\mathbf{L}_{h1}(\phi_1)\mathbf{n}_1(s_p,\theta_p,\psi_1) \tag{62}$$

$$\mathbf{n}_h^{(2)}(u_g,\theta_g,\phi_2)=\mathbf{L}_{hb_2}\mathbf{L}_{b_2 2}(\phi_2)\mathbf{n}_2(u_g,\theta_g) \tag{63}$$

Here:

$$\mathbf{L}_{h1}=\begin{bmatrix}\cos\phi_1 & \sin\phi_1 & 0\\ -\sin\phi_1 & \cos\phi_1 & 0\\ 0 & 0 & 1\end{bmatrix}$$

$$\mathbf{L}_{b_2 2} = \begin{bmatrix} \cos\phi_2 & -\sin\phi_2 & 0 \\ \sin\phi_2 & \cos\phi_2 & 0 \\ 0 & 0 & 1 \end{bmatrix}$$

$$\mathbf{L}_{hb_2} = \begin{bmatrix} \cos(\gamma+\Delta\gamma) & 0 & -\sin(\gamma+\Delta\gamma) \\ 0 & 1 & 0 \\ \sin(\gamma+\Delta\gamma) & 0 & \cos(\gamma+\Delta\gamma) \end{bmatrix}$$

Conditions of continuous tangency of pinion and gear tooth surfaces are represented by the following equations

$$\mathbf{r}_h^{(1)}(s_p,\theta_p,\psi_1,\phi_1) - \mathbf{r}_h^{(2)}(u_g,\theta_g,\phi_2) = \mathbf{0} \tag{64}$$

$$\mathbf{n}_h^{(1)}(s_p,\theta_p,\psi_1,\phi_1) - \mathbf{n}_h^{(2)}(u_g,\theta_g,\phi_2) = \mathbf{0} \tag{65}$$

$$f_{1p}^{(a)}(s_p,\theta_p,\psi_1) = 0 \tag{66}$$

Surfaces Σ_1 and Σ_2 are represented in S_h by four and three related parameters, respectively. Equation (66) is the equation of meshing of the pinion and generating head-cutter and relates the surface parameters of the head-cutter with the generalized parameter ψ_1 of motion of the process of generation of the pinion. Vector equations (64) , (65) and (66) yield three, two independent and one scalar equations, respectively. The whole system of equations (64) – (66) provides six equations for determination of seven unknowns represented as

$$f_i(s_p,\theta_p,\psi_1,\phi_1,u_g,\theta_g,\phi_2) = 0, \quad f_i \in C^1, \quad (i = 1,...,6) \tag{67}$$

One of the unknowns, say ϕ_1, is considered as the input parameter in the range $-\left(\frac{\pi}{N_1}\right) \le \phi_1 \le \left(\frac{\pi}{N_1}\right)$. It is assumed that the Jacobean of the system (67) differs from zero at each iteration.

The paths of contact on the pinion and the gear tooth surfaces are represented by the following functions:

$$\mathbf{r}_1 = \mathbf{r}_1(s_p(\phi_1),\theta_p(\phi_1),\psi_1(\phi_1)) \tag{68}$$

$$f_{1p}^{(a)}(s_p(\phi_1),\theta_p(\phi_1),\psi_1(\phi_1)) = 0 \tag{69}$$

and

$$\mathbf{r}_2 = \mathbf{r}_2(u_g(\phi_1),\theta_g(\phi_1)) \tag{70}$$

respectively.

The function of transmission errors is defined as

$$\Delta\phi_2(\phi_1) = \phi_2(\phi_1) - \frac{N_1}{N_2}\phi_1 \tag{71}$$

The bearing contact is formed as a set of instantaneous contact ellipses. The lengths of the major and minor axes of contact ellipse and their orientation are determined using the approach proposed in [8].

Using vector function (70), we may determine projection L_T of the path of contact on the gear tooth surface on the tangent plane at the mean contact point M. The goal is to obtain L_T as a straight line directed longitudinally. The process of computation is an iterative process and requires simultaneous application of local synthesis and TCA. The errors of alignment in this procedure are not taken into account. The influence of errors of alignment on transmission errors requires additional application of TCA.

It may be discovered in some cases of design, that the gear drive is too sensitive to errors of alignment. Then, it becomes necessary to deviate L_T from the longitudinal directed straight line by correction η_2 in procedure 3 (see Flow chart of Fig. 18).

8. Numerical Example

The theory developed will now be illustrated with the numerical example. The algorithms described above have been implemented by the computer program developed in Fortran and Visual Basic languages.

The blank data and gear machine-tool settings have been adapted from the Gleason summary and represented in Tables 2 and 3.

The final machine-tool settings for pinion generation have been determined as the output of the computer programs developed and are shown in Table 4. The results of TCA obtained by the developed computer programs are shown by Figs. 23, 24, 25, 26, and 27 for aligned and misaligned gear drives.

The investigation accomplished confirms that the longitudinal path of bearing contact developed is stabilized and the predesigned parabolic function absorbs the transmission errors caused by misalignment. The magnitude of transmission errors caused by misalignment might be controlled and does not exceed 7 arc seconds in the example.

Table 2: Blank Data

Applied parameters	Pinion	Gear
Number of teeth N_1, N_2	10	52
Shaft angle γ	90°	
Mean spiral angle β_1, β_2	32°30'	32°30'
Hand of spiral	Right hand	Left hand
Whole depth (mm)	16.637	16.637
Pitch angles γ_1, γ_2	10°53'	79°7'
Root angles $\gamma_{r_1}, \gamma_{r_2}$	9°42'	75°8'
Face angles $\gamma_{f_1}, \gamma_{f_2}$	14°52'	80°18'
Addendum (mm)	11.811	3.429
Dedendum (mm)	4.826	13.208
Face width F_w (mm)	71.120	
Diametral pitch (1/inch)	3.156	
Clearance c_1, c_2 (mm)	1.400	
Mean cone distance A_m (mm)	177.521	

Table 3: Gear Machine Tool Settings and Installment of Head-Cutter

Applied parameters	Data
1. Blade Specifications	
Blade angle at mean point M	20°
Parabolic coefficient a_c	0.002
Cutter Radial R_{tt} (mm)	177.800
Cutter point radius R_g (mm)	177.800 ± 2.4123
Blade edge radius ρ_w (mm)	2.794
Point width P_{w_2} (mm)	4.826
Gear Machine-Tool Settings	
Machine root angle γ_{m_2}	$76^{\circ}10$
Machine center to back X_G (mm)	-2.007
Horizontal H_2 (mm)	100.152
Vertical V_2 (mm)	137.897

Table 4: Pinion Machine-Tool Settings and Blade Data

Applied parameters	Concave Side	Convex Side
Blade angle α_p	17°	23°
Cutter point radius R_p (mm)	174.496	185.151
Radial setting S_{r_1} (mm)	150.301	195.018
Installment angle q_1	$62^{\circ}3'45''$	$61^{\circ}32'12''$
Machine center to back X_{D_1} (mm)	-4.530	8.134
Sliding base X_{B_1} (mm)	0.339	-1.795
Blank offset E_{m_1} (mm)	19.947	-20.314
Ratio of cutting m_{1p}	4.853	5.773
Machine root angle γ_{m_1}	9.7°	9.7°
Coefficient of modified roll b_2	0.0302	-0.0527
Coefficient of modified roll b_3	-0.0599	0.1157

9. Conclusion

Based on the research performed the following conclusions can be drawn:

(1) The developed approach of design has been successfully applied and enabled to design formate cut spiral bevel gears with a stabilized bearing contact and favorable shape of transmission errors of low magnitude.

(2) The theoretical results obtained have been confirmed by simulation of meshing.

References

1 Litvin, F.L. Rahman P. and Goldrich R.N. 1982, "Mathematical Models for the Synthesis and Optimization of Spiral Bevel Gear Tooth Surfaces", *NASA CR-3553.*

2 Litvin, F.L. and Zhang, Y. 1991, "Local Synthesis and Tooth Contact Analysis of Face-Milled Spiral Bevel Gears", *NASA Contractor Report 4342*, AVSCOM Technical Report 90-C-028

3 Lewicki, D.G., Handschuh, R.F., Henry, Z.S. and Litvin, F.L., 1994, "Low-Noise, High-Strength, Spiral-Bevel Gears for Helicopter Transmissions", *Journal of Propulsion and Power*, Vol. 10, No. 3.

4 Litvin, F.L. and Zhao, X. 1996, "Computerized Design and Analysis of Face-milled, Uniform Tooth Height, Low-Noise Spiral Bevel Gear Drives", *NASA Contractor Report 4704.*

5 Litvin, F.L., Wang, A.G., and Handschuh R.F. 1996, "Computerized Design and Analysis of FaceMilled, Uniform Tooth Height Spiral Bevel Gear Drives", *Journal of Mechanical Design*, Vol. 118, pp. 573-579.

6 Zhang, Y., Litvin, F.L., and Handschuh R.F. 1995, "Computerized Design of Low-Noise Face-Milled Spiral Bevel Gears", *Mech. Mach. Theory,* Vol. 30, No. 8, pp. 1171-1178.

7 F. L. Litvin, A. G. Wang and R. F. Handschuh, Computerized generation and simulation of meshing and contact of spiral bevel gears with improved geometry, *J. Comput. Methods Appl. Mech. Engrg.* , 158 (1998) 35-64.

8 Litvin, F.L. 1994, *Gear Geometry and Applied Theory*, Prentice Hall.

9 Litvin, F.L. 1960, 1968, *Theory of Gearing,* 1st ed. (1960), 2nd ed. (1968). Nauka (in Russian).

10 Zalgaller, V.A. 1975, *Theory of Envelopes*, Nauka, Moscow (in Russian)

11 IMSL Fortran 90 MP Library, v. 3.0, *Visual Numerics, Inc.*,1998

12 Press, William H., et al, Numerical Recipes in Fortran 77, *The Art of Scientific Computing,* Cambridge University Press, New York, 2nd Edition, 1992.

13 Litvin, F.L. 1969, "Die Beziehungen Zwischen den Krummungen der Zahnoberflachen bei Raumlichen Verzahnungen". *Z. Angew. Math. Mech.* 49: 685-690 (in German).

14 Litvin, F.L. 1989, *Theory of Gearing,* NASA Reference Publication 1212.

Appendix 1:—Relationships Between Principal Curvatures and Directions of Mating Surfaces

Introduction

The procedure of local synthesis requires the knowledge of principal curvatures and directions of contacting surfaces. In the case of design discussed in this paper, the pinion tooth surface is represented by three related parameters and the determination of pinion principal curvatures and directions is a complex problem. The solution to the problem is simplified by representation of pinion principal curvatures and directions in terms of principal curvatures and directions of the head-cutter and parameters of motions of the generating process (proposed in [8, 13]).

Important relations between principal curvatures and directions of mating surfaces in point contact (proposed in [8, 13]) are applied for local synthesis (see section 6).

Henceforth two types of instantaneous contact of meshing surfaces will be considered: (i) along a line, and (ii) at a point. Line contact is provided in meshing of the surface being generated with the tool surface. Point contact is provided for the generated pinion and gear tooth surfaces. The determination of the required relationships is based on the approach proposed in [8, 14]. The basic equations in the approach developed are as follows

$$\mathbf{v}_r^{(2)} = \mathbf{v}_r^{(1)} + \mathbf{v}^{(12)} \tag{72}$$

$$\dot{\mathbf{n}}_r^{(2)} = \dot{\mathbf{n}}_r^{(1)} + \boldsymbol{\omega}^{(12)} \times \mathbf{n} \tag{73}$$

$$\frac{d}{dt}\left[\mathbf{n} \cdot \mathbf{v}^{(12)}\right] = 0 \tag{74}$$

Equations (72) and (73) relate the velocities of the contact point and the tip of the unit normal in their motions over the contacting surfaces. Equation (74) represents the differentiated equation of meshing. Equations (72)-(74) yield a skew-symmetric system of three linear equations in two unknowns x_1 and x_2 of the following structure

$$a_{i_1} x_1 + a_{i_2} x_2 = a_{i_3} \qquad (i=1-3) \tag{75}$$

Here: x_1 and x_2 are the projections of the velocity of the contact point in the motion over one of the surface on the principal directions of the mating surface. In case of line contact of surfaces the solution for the unknowns is indefinite and the rank of the system matrix of the linear equations is one. In case of point contact of surfaces the solution for the unknowns is definite, and the rank of the system matrix is two. The properties mentioned above are used for the derivation of the sought for relationships between the principal curvatures and directions of the meshing surfaces.

Meshing of Surfaces Σ_1 and Σ_2: Surfaces Σ_1 and Σ_2 are in point contact and their meshing is considered in fixed coordinate system S_l (Fig. 20). Equations (72)-(74) yield the following system of three linear equations [8, 14]

$$a_{i_1} v_s^{(1)} + a_{i_2} v_q^{(1)} = a_{i_3}, \ (i=1-3) \tag{76}$$

where

$$v_s^{(1)} = \mathbf{v}_r^{(1)} \cdot \mathbf{e}_s \ , \quad v_q^{(1)} = \mathbf{v}_r^{(1)} \cdot \mathbf{e}_q \tag{77}$$

$$\left.\begin{aligned}
a_{11} &= k_s - k_f \cos^2\sigma^{(12)} - k_h \sin^2\sigma^{(12)} \\
a_{12} &= a_{21} = 0.5(k_f - k_h)\sin 2\sigma^{(12)} \\
a_{13} &= a_{31} = -k_s v_s^{(12)} + [(\mathbf{n}\times\boldsymbol{\omega}^{(12)})\cdot\mathbf{e}_s] \\
a_{22} &= k_q - k_f \sin^2\sigma^{(12)} - k_h \cos^2\sigma^{(12)} \\
a_{23} &= a_{32} = -k_q v_q^{(12)} + [(\mathbf{n}\times\boldsymbol{\omega}^{(12)})\cdot\mathbf{e}_q] \\
a_{33} &= k_s (v_s^{(12)})^2 + k_q (v_q^{(12)})^2 - [(\mathbf{n}\times\boldsymbol{\omega}^{(12)})\cdot\mathbf{v}^{(12)}] \\
&-\mathbf{n}\cdot[(\boldsymbol{\omega}^{(1)}\times\mathbf{v}_{\mathbf{tr}}^{(2)}) - (\boldsymbol{\omega}^{(2)}\times\mathbf{v}_{\mathbf{tr}}^{(1)})] + m_{21}^{'}(\mathbf{n}\times\mathbf{k}_2)\cdot\mathbf{r}
\end{aligned}\right\} \tag{78}$$

The following are considered as being known: point M of tangency of surfaces Σ_1 and Σ_2, the common surface unit normal, the relative velocity $\mathbf{v}^{(12)}$, the principal curvatures k_s and k_q and directions $\mathbf{e_s}$ and $\mathbf{e_q}$ on Σ_2 at M, and the elastic deformation δ of surfaces at M. The goal is to determine the principal curvatures k_f and k_h and the angle $\sigma^{(12)}$ formed by the unit vectors $\mathbf{e_f}$ and $\mathbf{e_s}$.

The velocity $\mathbf{v}_\mathbf{r}^{(i)}$ (i=*1, 2*) of the contact point on surface Σ_i has a definite direction and therefore the rank of the system matrix (76) is one. This property yields the following relation:

$$\begin{vmatrix} a_{11} & a_{12} & a_{13} \\ a_{21} & a_{22} & a_{23} \\ a_{31} & a_{32} & 33 \end{vmatrix} = F(k_f, k_h, k_s, k_q, \sigma^{(12)}, m_{21}^{'}) = 0 \tag{79}$$

The sought for solution for k_f, k_h and $\sigma^{(12)}$ can be obtained if the following parameters will be chosen: the derivative $m_{21}^{'}$; the ratio a/δ, where a is the major axis of the contact ellipse; the direction at M of the tangent to the contact path on one of the contacting surfaces Σ_1 and Σ_2. The relation between the directions at M of the tangents to the contact paths on both surfaces is represented by the equation [8, 14]

$$\tan\eta_1 = \frac{-a_{13}v_q^{(12)} + (a_{33} + a_{13}v_s^{(12)})\tan\eta_2}{a_{33} + a_{23}(v_q^{(12)} - v_s^{(12)}\tan\eta_2)} \tag{80}$$

Choosing η_2 at point M, we can determine η_1.

Procedure of Determination of k_f, k_h and $\sigma^{(12)}$

Step 1: Determine η_1 choosing η_2.

Step 2:

$$v_s^{(1)} = \frac{a_{33}}{a_{13} + a_{23}\tan\eta_1} \tag{81}$$

$$v_q^{(1)} = \frac{a_{33}\tan\eta_1}{a_{13} + a_{23}\tan\eta_1} \tag{82}$$

Step 3:

$$A = \frac{\delta}{a^2} \tag{83}$$

Step 4:

$$K_\Sigma = \frac{\dfrac{a_{13}^2 + a_{23}^2}{(v_s^{(1)})^2 + (v_q^{(1)})^2} - 4A^2}{\dfrac{a_{13}v_s^{(1)} + a_{23}v_q^{(1)}}{(v_s^{(1)})^2 + (v_q^{(1)})^2} + 2A} \tag{84}$$

Step 5:

$$\begin{bmatrix} a_{11} \\ a_{12} \\ a_{22} \end{bmatrix} = \frac{1}{(v_s^{(1)})^2 + (v_q^{(1)})^2} \begin{bmatrix} a_{13}v_s^{(1)} - a_{23}v_q^{(1)} + (v_q^{(1)})^2 K_\Sigma \\ a_{13}v_q^{(1)} + a_{23}v_s^{(1)} - v_s^{(1)}v_q^{(1)} K_\Sigma \\ -a_{13}v_s^{(1)} + a_{23}v_q^{(1)} + (v_s^{(1)})^2 K_\Sigma \end{bmatrix} \tag{85}$$

Step 6:

$$\tan 2\sigma^{(12)} = \frac{2a_{12}}{g_2 - (a_{11} - a_{22})} \tag{86}$$

where $g_2 = k_s - k_q$.

Step 7:

$$g_1 = \frac{2a_{12}}{\sin 2\sigma^{(12)}} \tag{87}$$

Step 8:

$$K_\Sigma^{(1)} = K_\Sigma^{(2)} - K_\Sigma \tag{88}$$

where $K_\Sigma^{(2)} = k_s + k_q$.

Step 9:

$$k_f = (K_\Sigma^{(1)} + g_1)/2 \tag{89}$$

Step 10:

$$k_h = (K_\Sigma^{(1)} - g_1)/2 \tag{90}$$

The procedure provided above can be used to obtain the sought for principal curvatures k_f and k_h at point M of tangency of surfaces Σ_1 and Σ_2 and the principal directions on Σ_1 at M.

Meshing of Surfaces Σ_1 and Σ_p: The tool surface Σ_p generates the pinion tooth surface Σ_1. Surfaces Σ_1 and Σ_p are in line contact and point B is the given point of the instantaneous line of contact. The meshing of surfaces is considered in S_{m_1}. At point B the following are assumed as given: the curvatures k_f and k_h of surface Σ_p; the unit vectors $\mathbf{e}_f$ and $\mathbf{e}_h$ of principal directions on Σ_1; the surfaces unit normal ; the relative velocity $\mathbf{v}^{(12)}$. The goal is to determine the principal curvatures k_p and k_t of surface Σ_p, and the angle $\sigma^{(1p)}$ that is formed by the unit vectors $\mathbf{e}_f$ and $\mathbf{e}_p$.

Equation (72)-(74) yield a system of three linear equations

$$d_{i1}v_f^{(p)} + d_{i2}v_h^{(p)} = d_{i3} \quad (i=1-3) \tag{91}$$

where

$$v_f^{(p)} = \mathbf{v}_r^{(p)} \cdot \mathbf{e}_f \ , \ v_h^{(p)} = \mathbf{v}_r^{(p)} \cdot \mathbf{e}_h \tag{92}$$

The direction of $\mathbf{v}_r^{(p)}$ is indefinite since surfaces Σ_p and Σ_1 are in line contact. Therefore, the rank of system matrix of equations is equal to one. Using this property, the following equations are obtained:

$$\left.\begin{aligned} \tan 2\sigma^{(1p)} &= \frac{-2d_{13}d_{23}}{d_{23}^2 - d_{13}^2 - (k_f - k_h)d_{33}} \\ k_t - k_p &= \frac{-2d_{13}d_{23}}{d_{33}\sin 2\sigma^{(1p)}} \\ k_t + k_p &= k_f + k_h + \frac{d_{13}^2 + d_{23}^2}{d_{33}} \end{aligned}\right\} \tag{93}$$

Here:

$$\left.\begin{aligned} d_{13} &= -k_f v_f^{(1p)} + [(\mathbf{n}\times\boldsymbol{\omega}^{(1p)})\cdot\mathbf{e}_f] \\ d_{23} &= -k_h v_h^{(12)} + [(\mathbf{n}\times\boldsymbol{\omega}^{(1p)})\cdot\mathbf{e}_h] \\ d_{33} &= -k_f (v_f^{(1p)})^2 - k_h (v_h^{(1p)})^2 - [(\mathbf{n}\times\boldsymbol{\omega}^{(1p)})\cdot\mathbf{v}^{(1p)}] \\ &- \mathbf{n}\cdot[(\boldsymbol{\omega}^{(1)}\times\mathbf{v}_{tr}^{(p)}) - (\boldsymbol{\omega}^{(p)}\times\mathbf{v}_{tr}^{(1)})] \end{aligned}\right\} \tag{94}$$

where

$$v_f^{(1p)} = \mathbf{v}^{(1p)} \cdot \mathbf{e}_f \ , \ v_h^{(1p)} = \mathbf{v}^{(1p)} \cdot \mathbf{e}_h \tag{95}$$

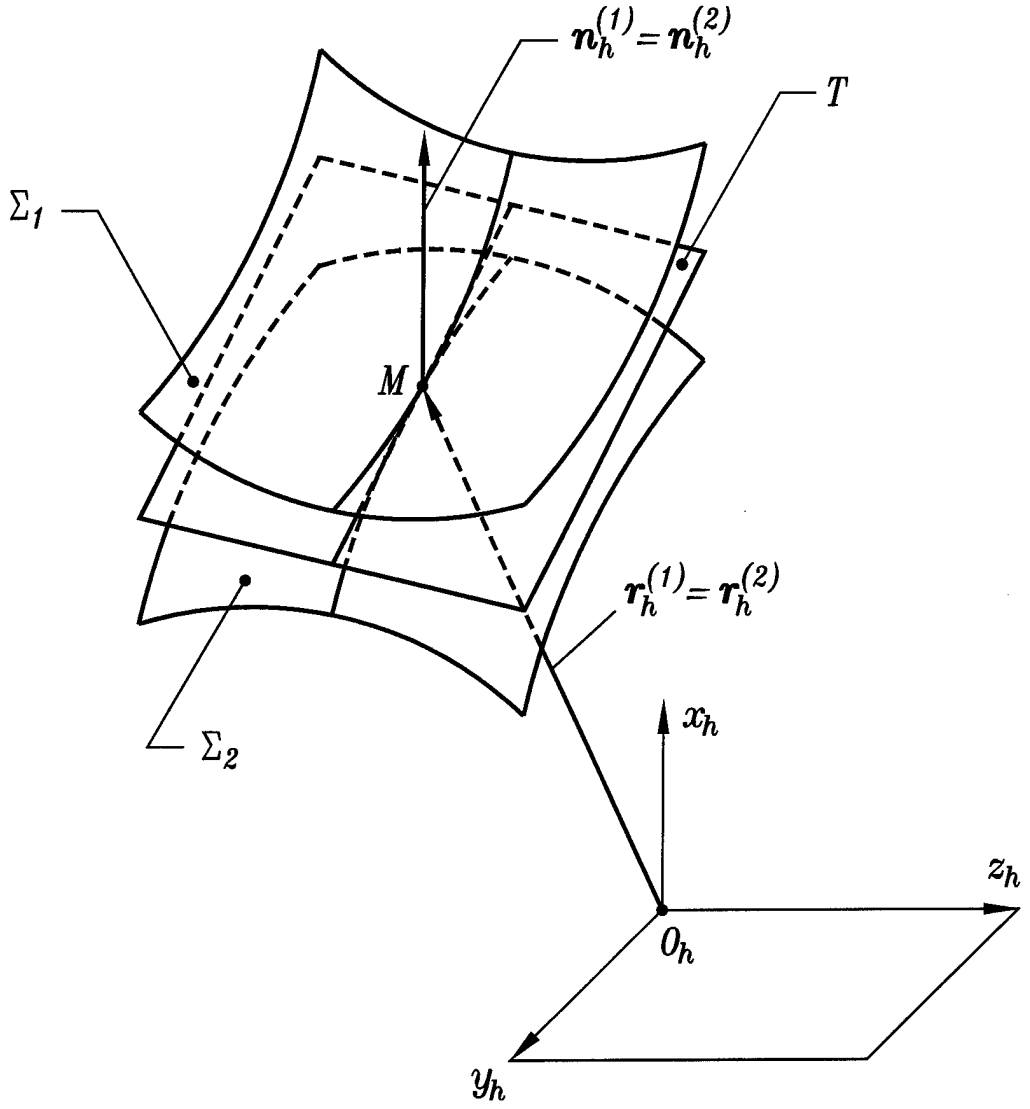

Figure 1.—Illustration of tangency of surfaces Σ_1 and Σ_2.

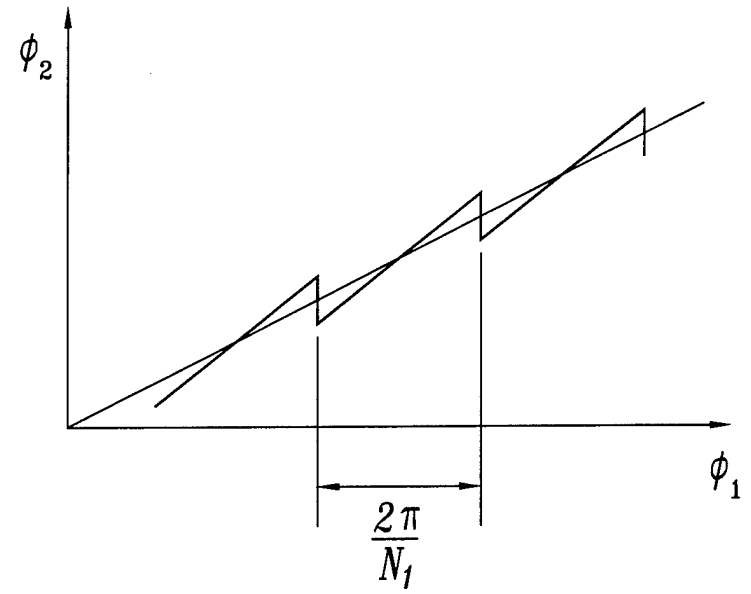

(a)

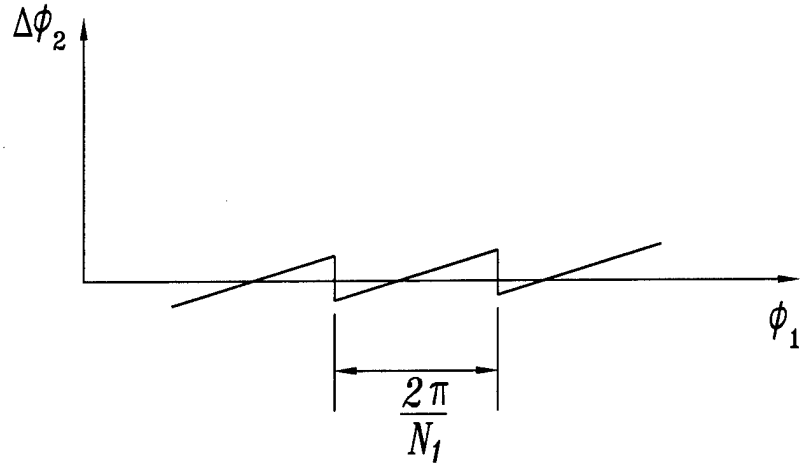

(b)

Figure 2.—Transmission function (a) and function of transmission errors (b) of a misaligned gear drive.

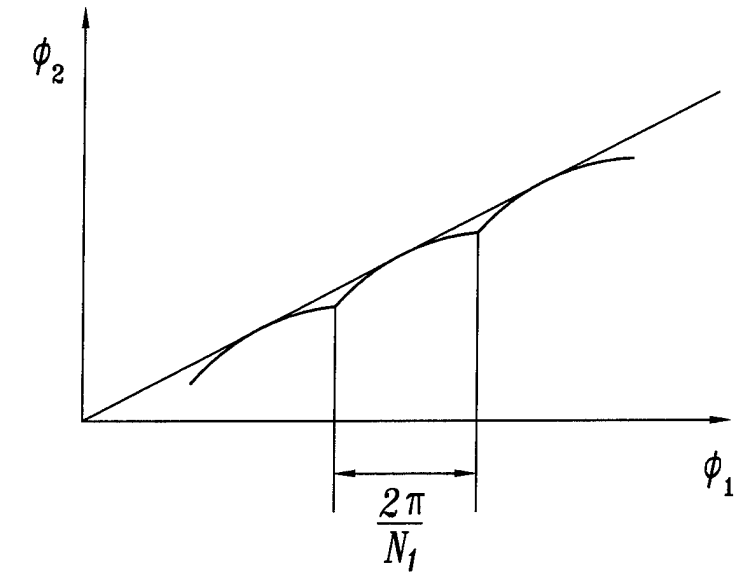

(a)

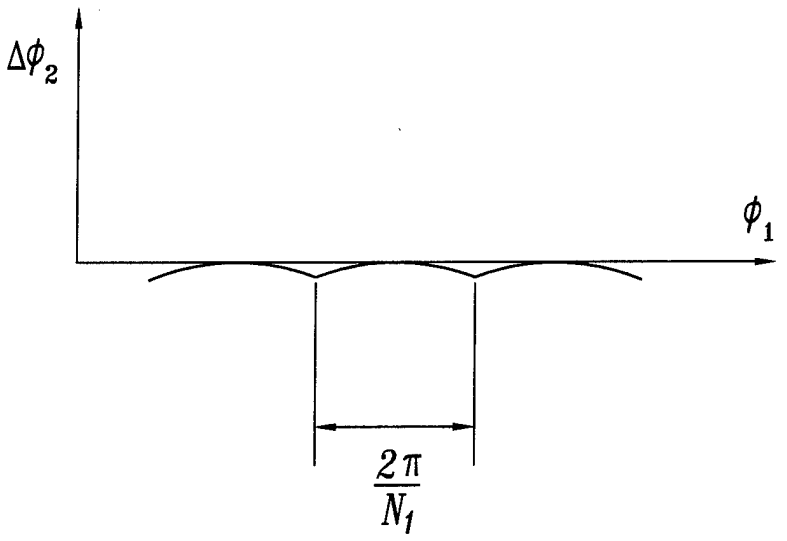

(b)

Figure 3.—Transmission function (a) and function of transmission errors (b) of a gear drive with a predesigned parabolic function.

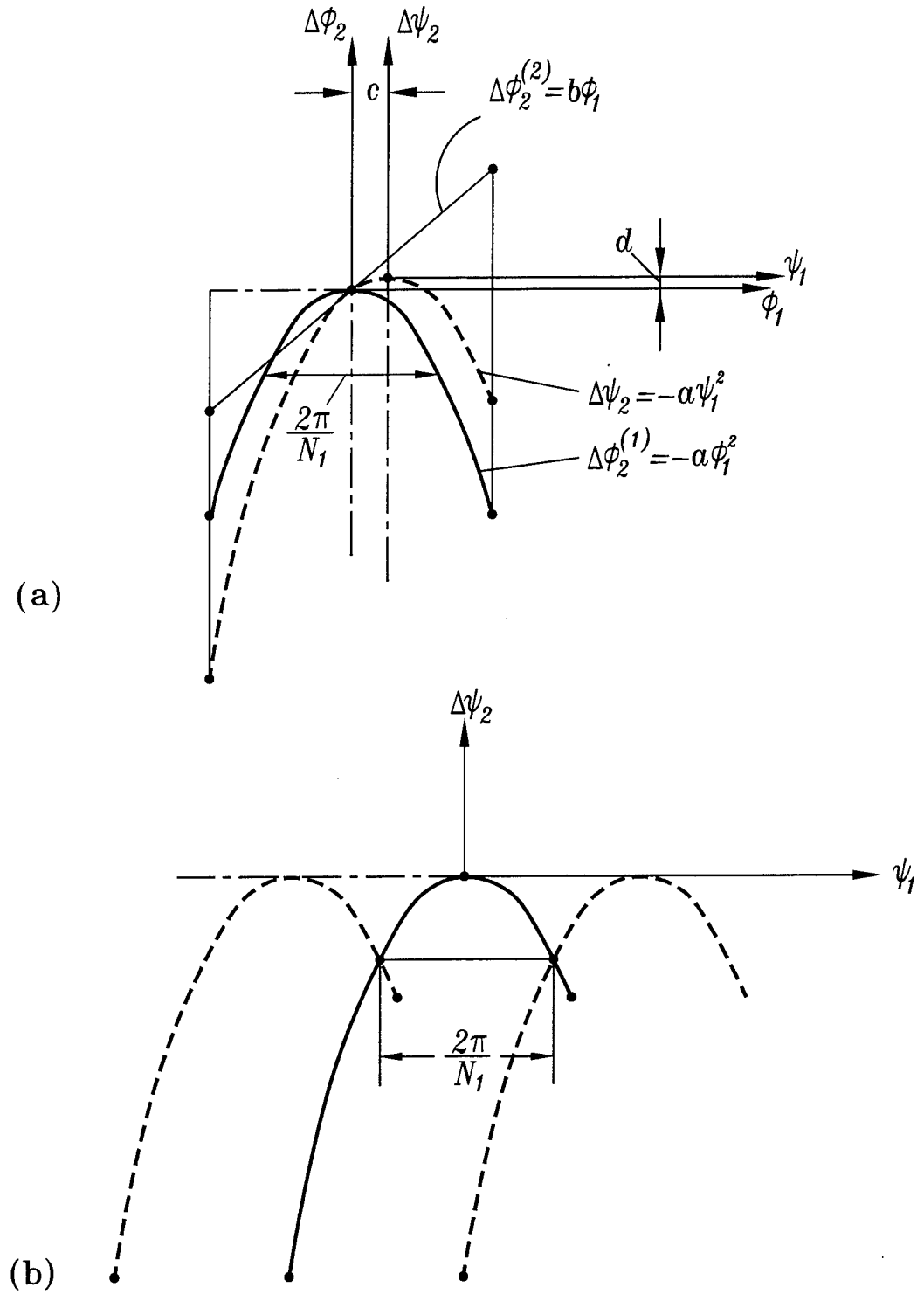

Figure 4.—Interaction of predesigned parabolic function $\Delta\phi_2^{(1)}(\phi_1)$ with linear function $\Delta\phi_2^{(2)}(\phi_1)$ caused by misalignment.

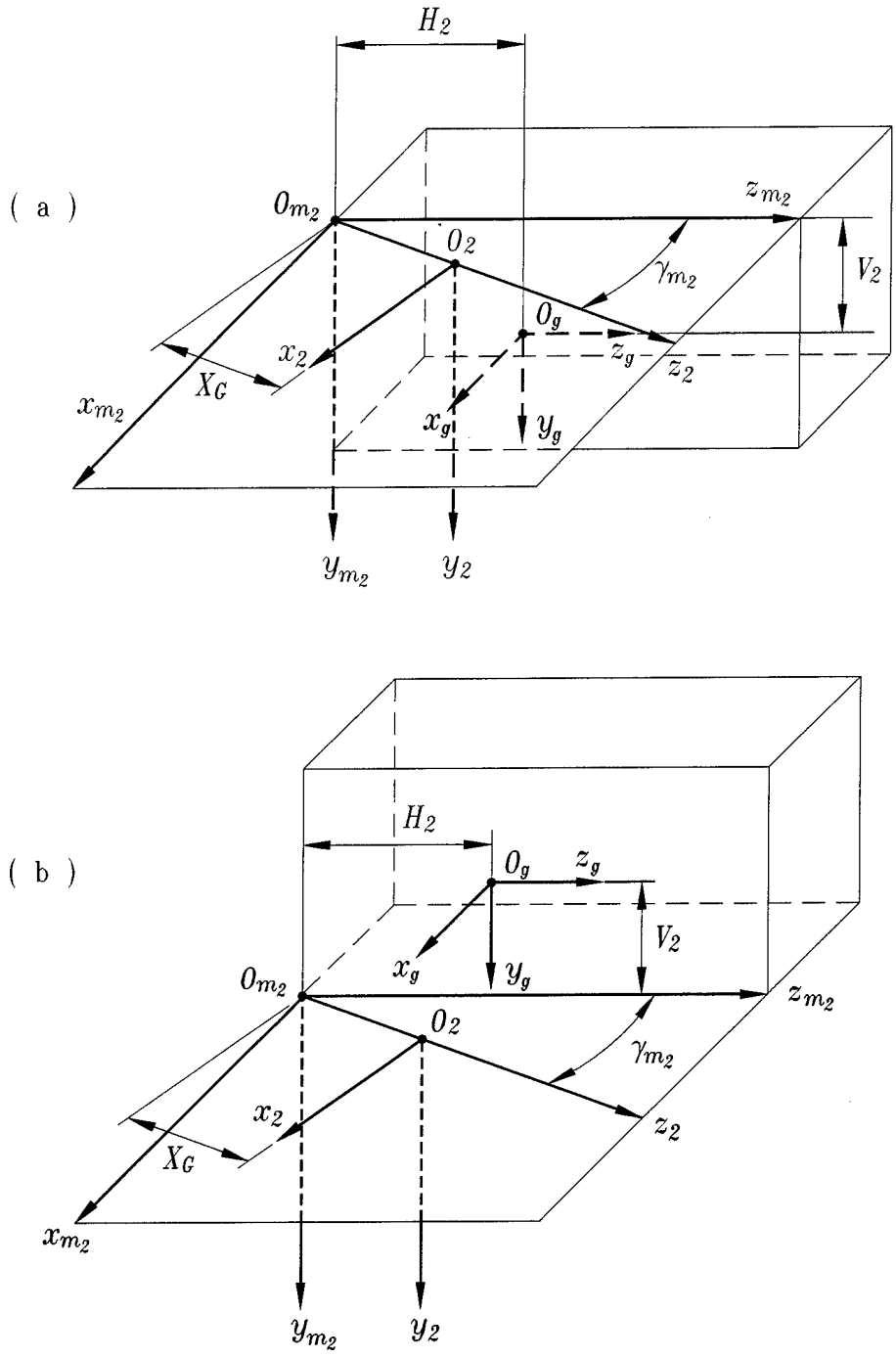

Figure 5.—Machine tool settings for gear generation. (a) For left hand gear. (b) For right hand gear.

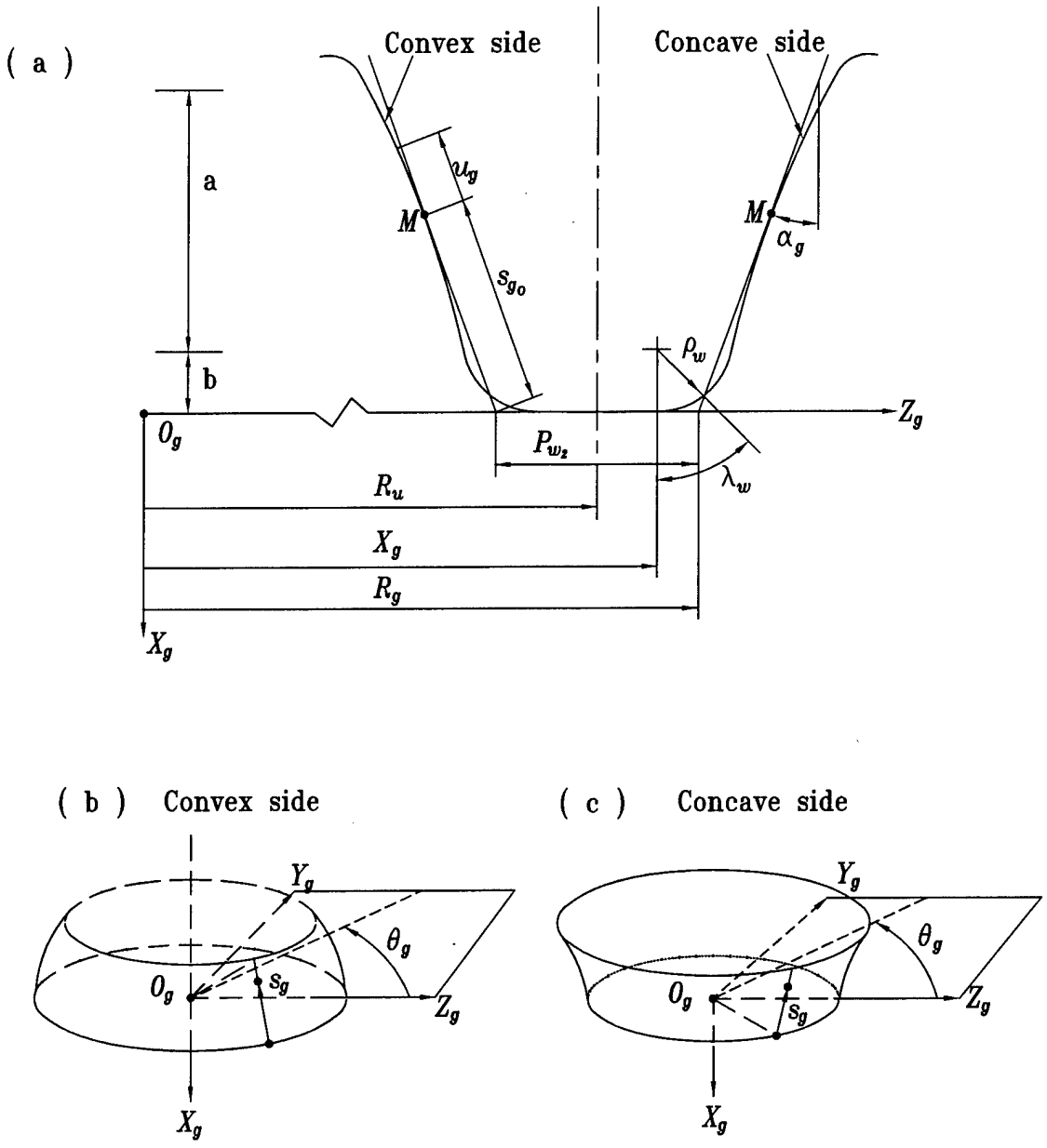

Figure 6.—Illustration of gear cutter blades and generating surfaces.

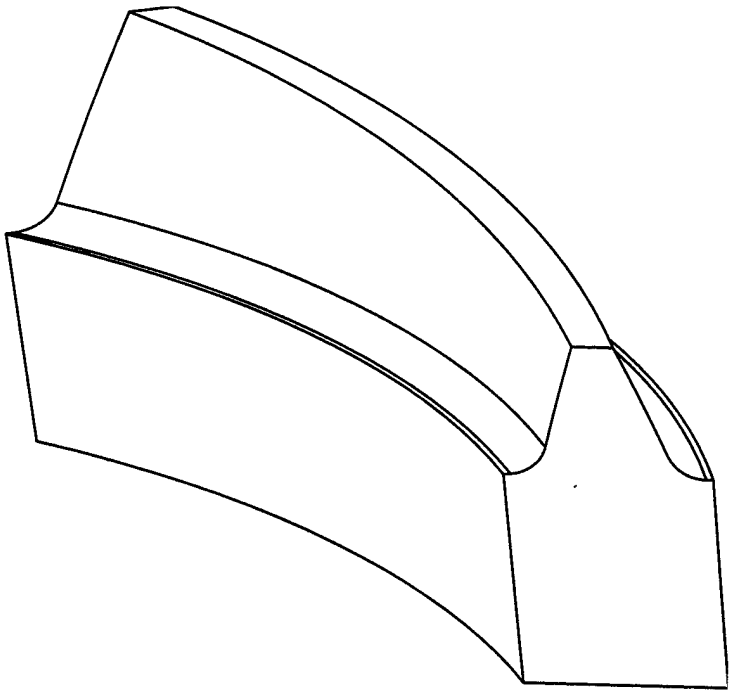

Figure 7.—Geometric model of gear tooth surfaces.

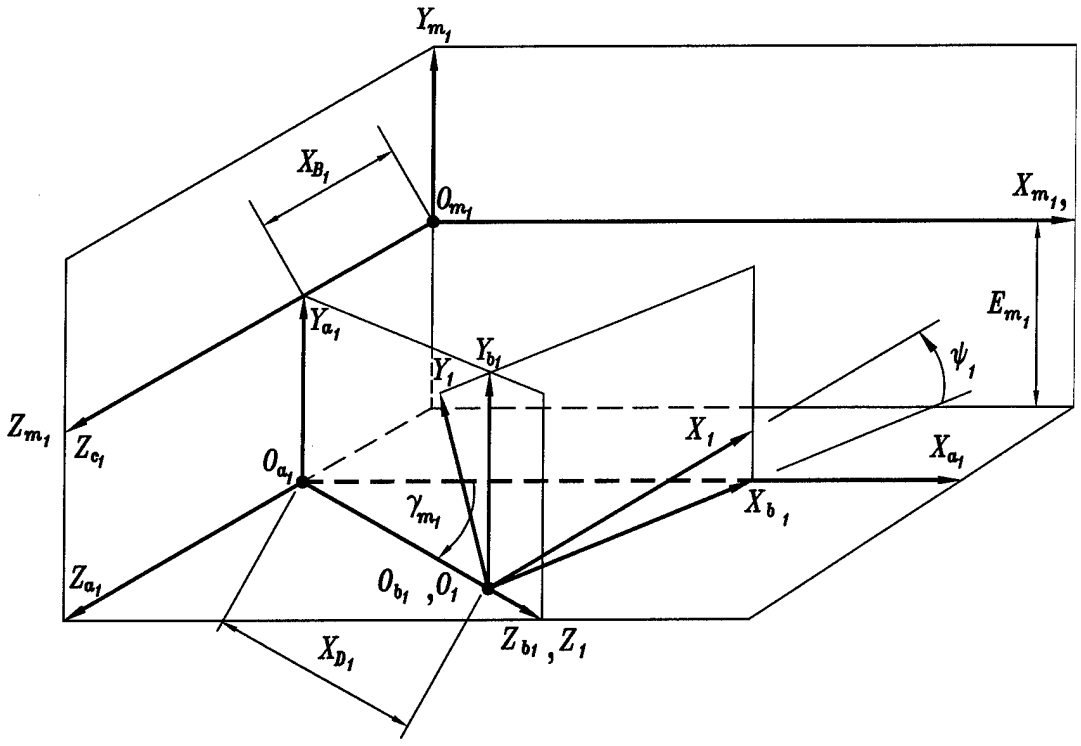

Figure 8.—Machine tool settings for installment of the to-be-generated pinion.

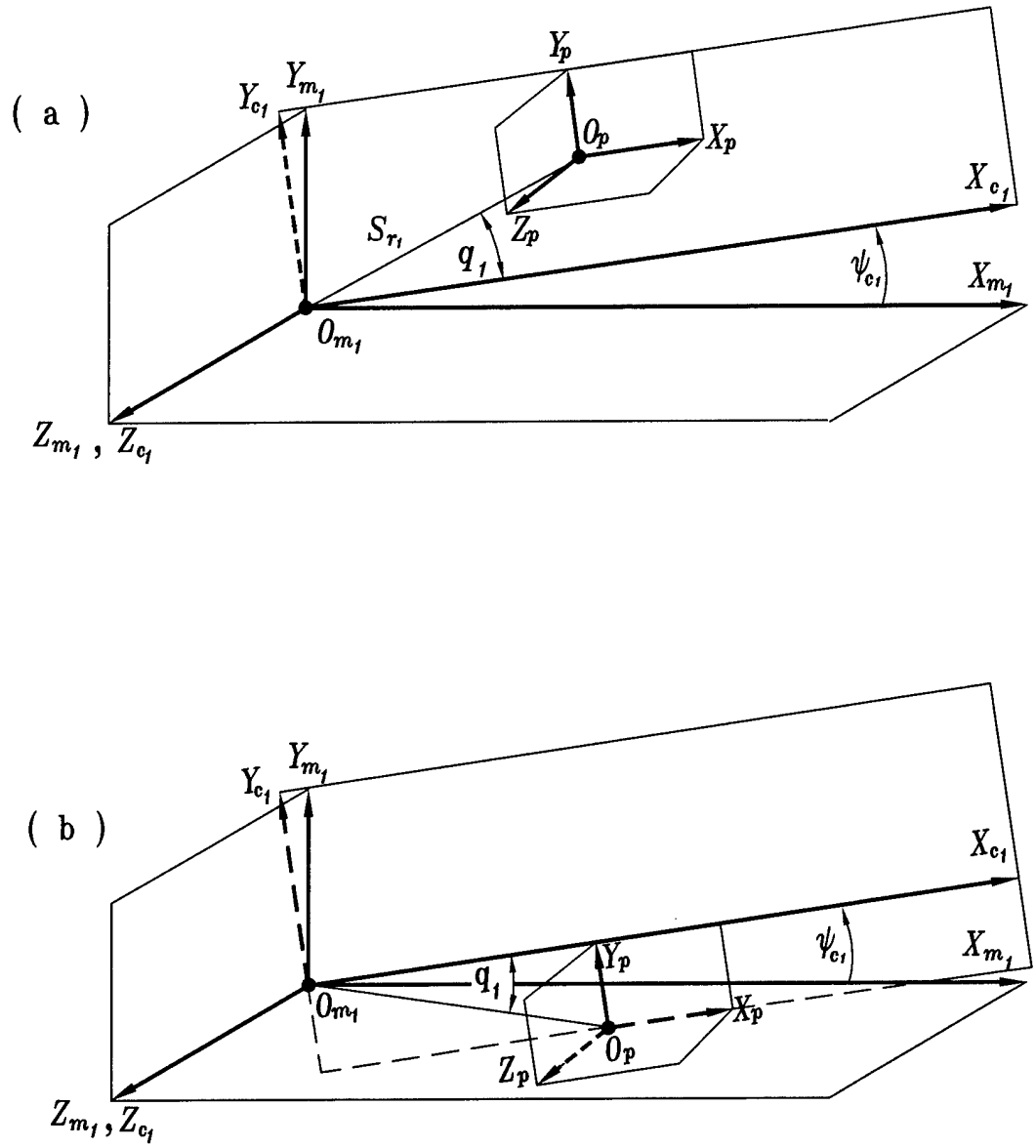

Figure 9.—Machine tool settings for installment of pinion head-cutter. (a) For right hand pinion. (b) For left hand pinion.

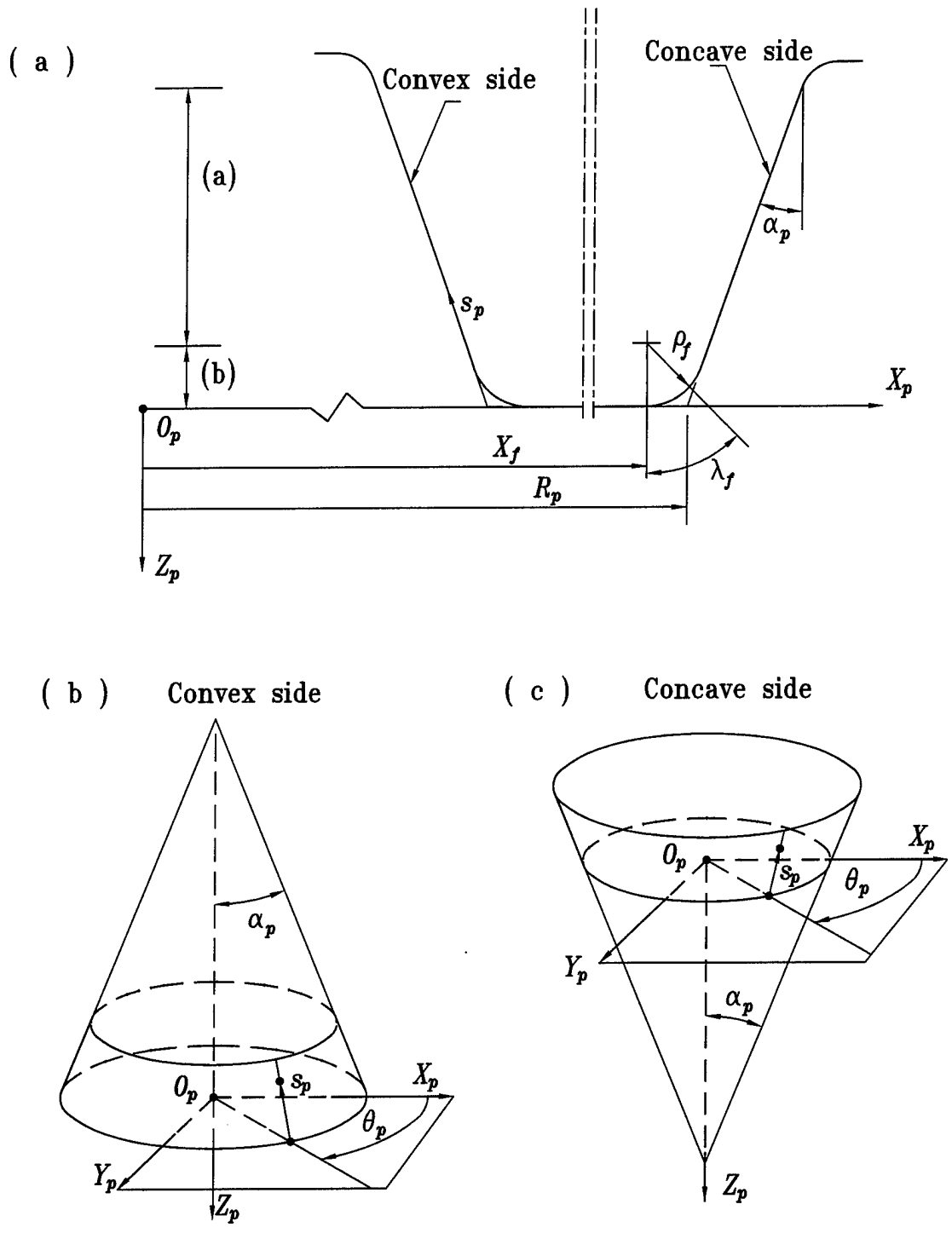

Figure 10.—Illustration of pinion cutter blades and generating surfaces.

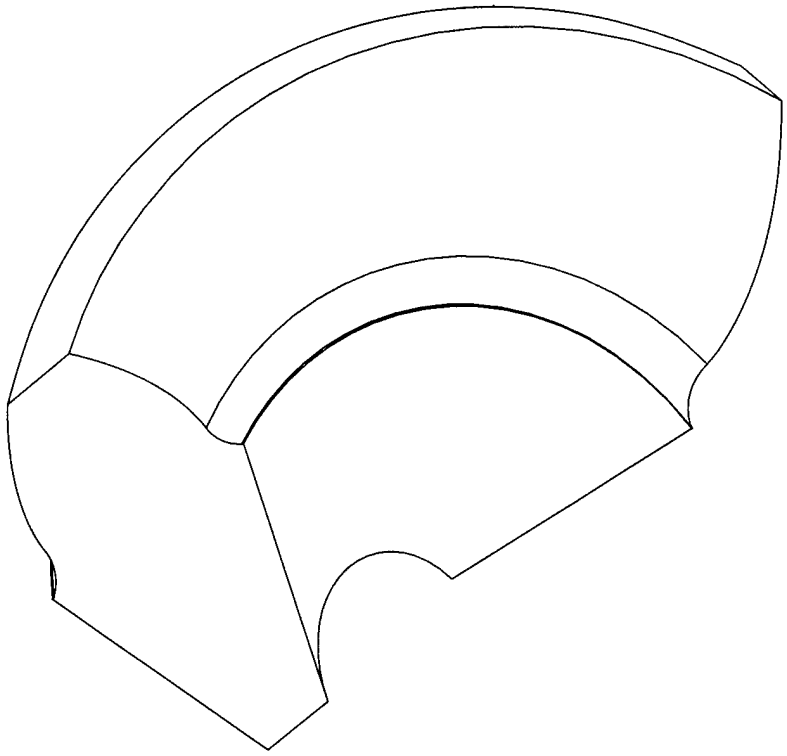

Figure 11.—Geometric model of pinion tooth surfaces.

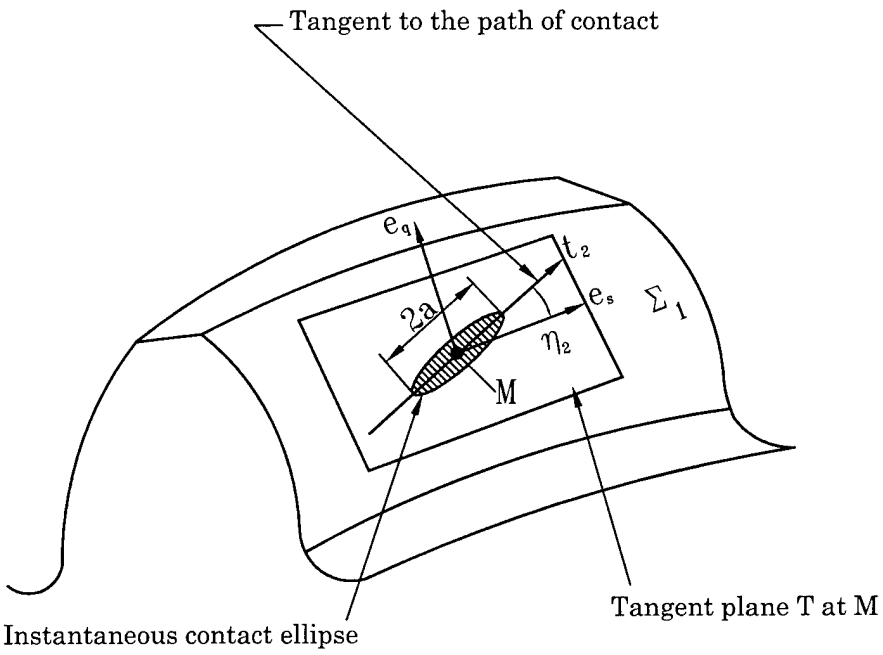

Figure 12.—Illustration of parameters η_2 and a applied for local synthesis.

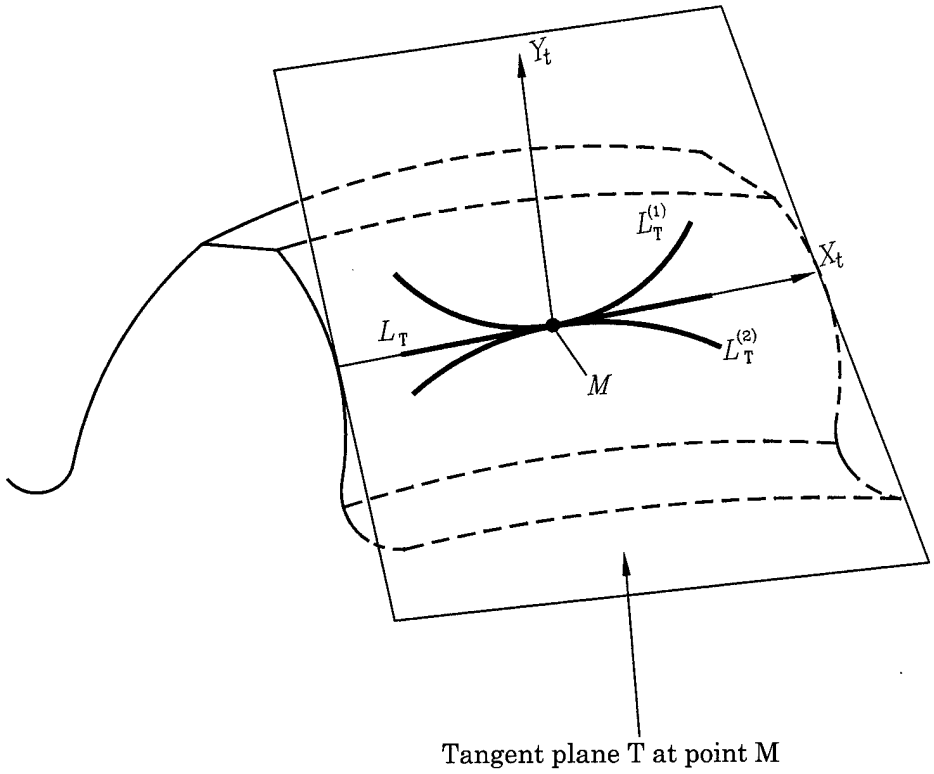

Figure 13.—Projections of various paths of contact L_T on tangent plane T.

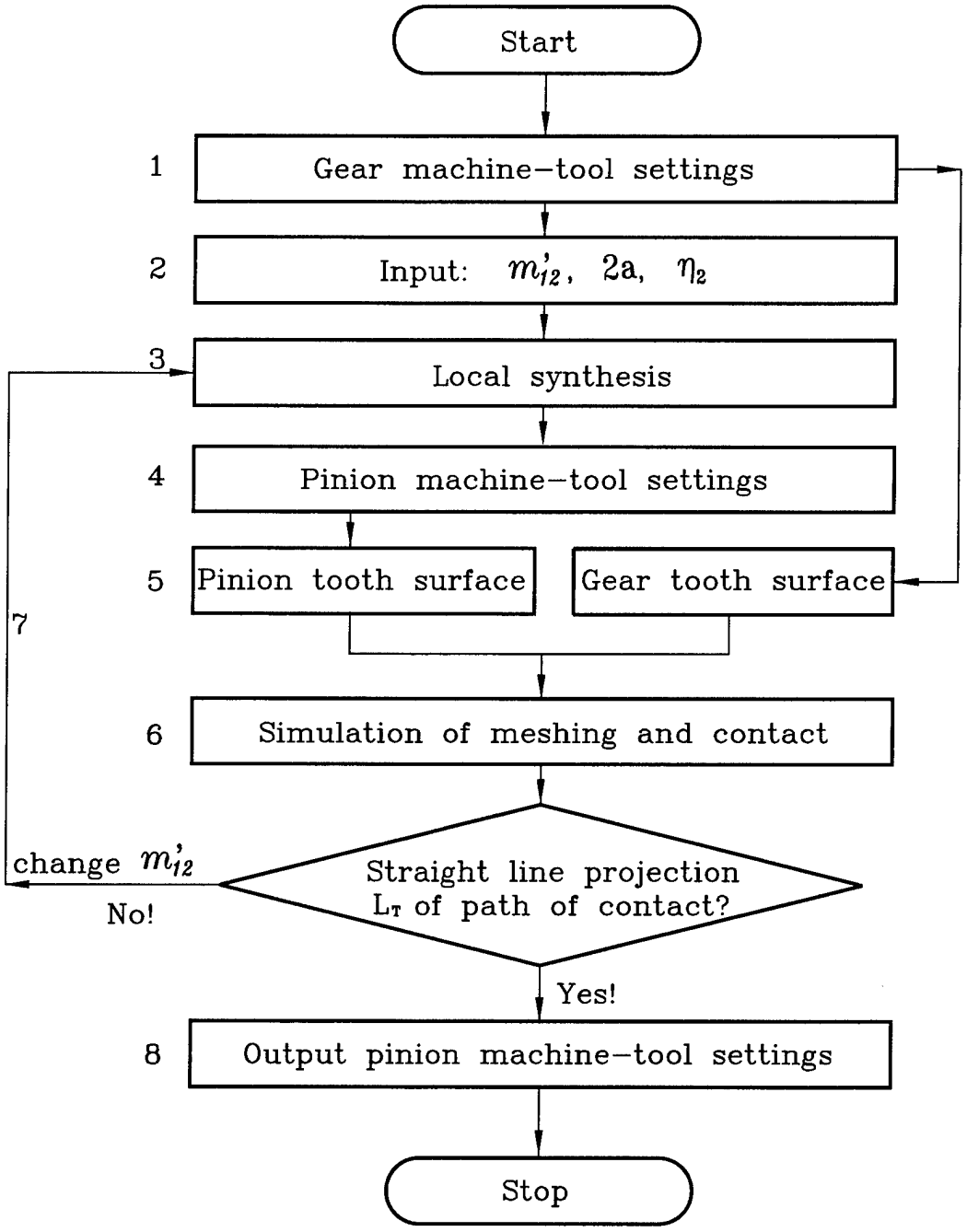

Figure 14.—Flow chart for procedure 1: design of bearing contact.

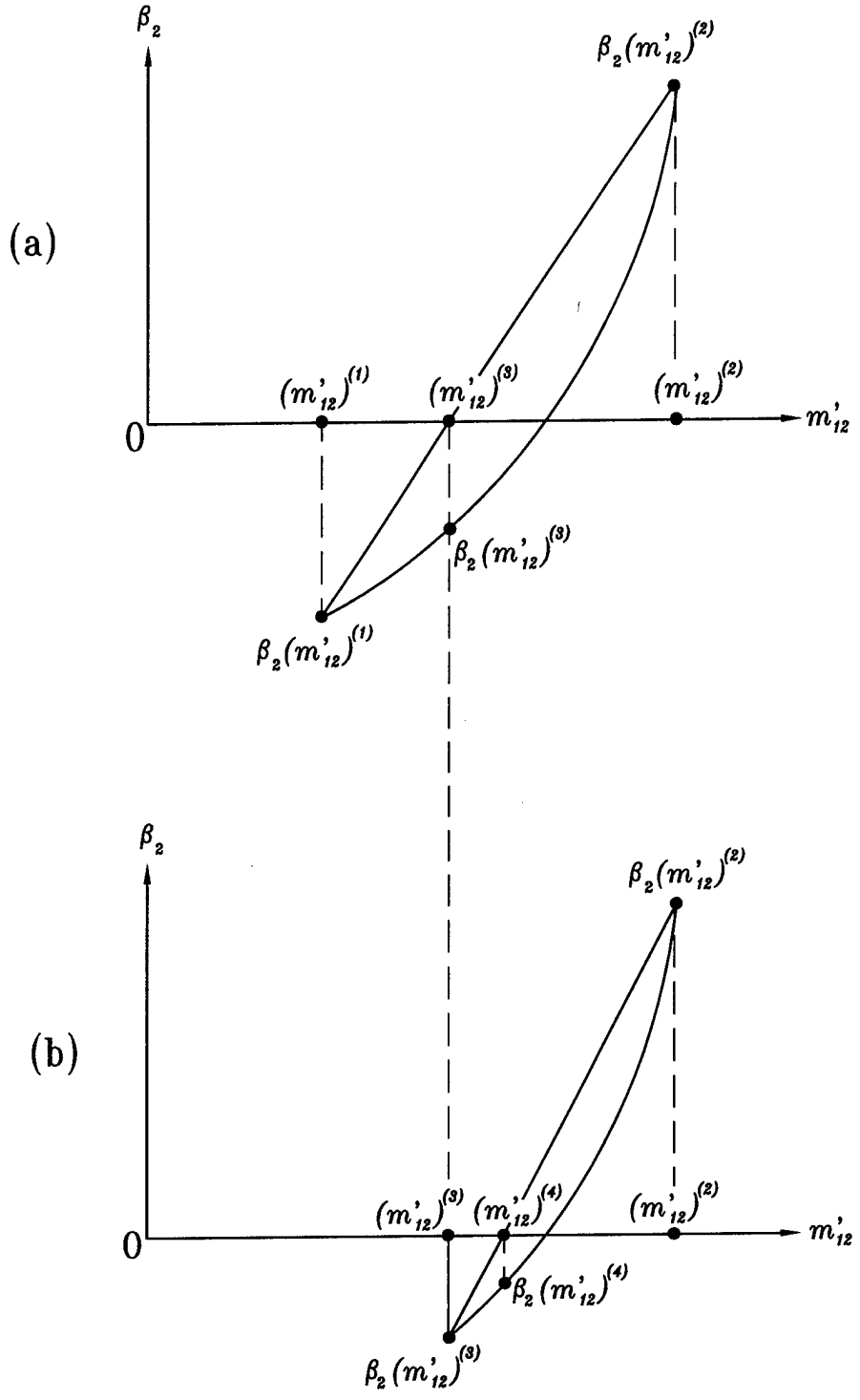

Figure 15.—Illustration of computations for determination of $\beta_2(m'_{12}) = 0$.

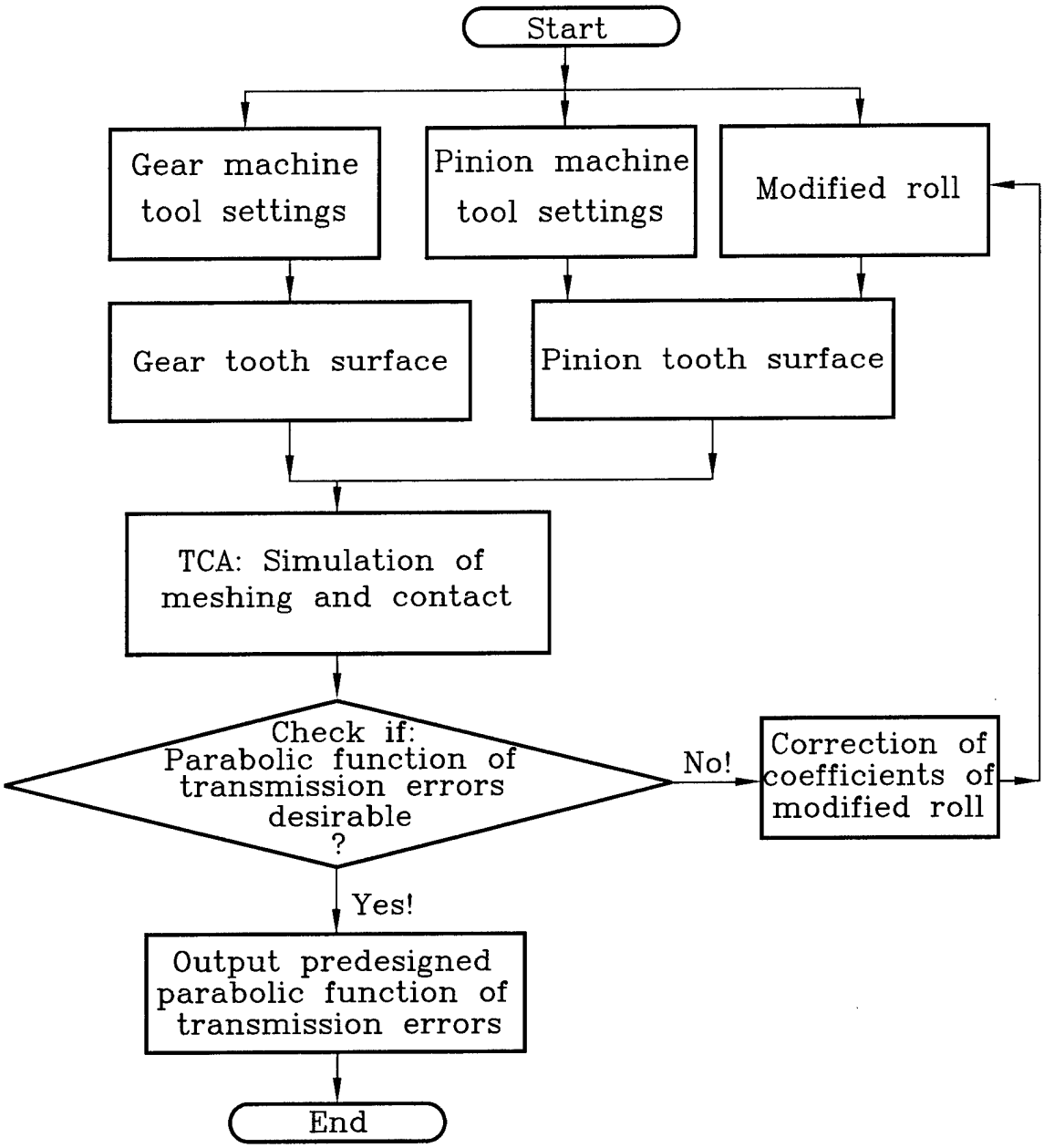

Figure 16.—Flow chart for procedure 2.

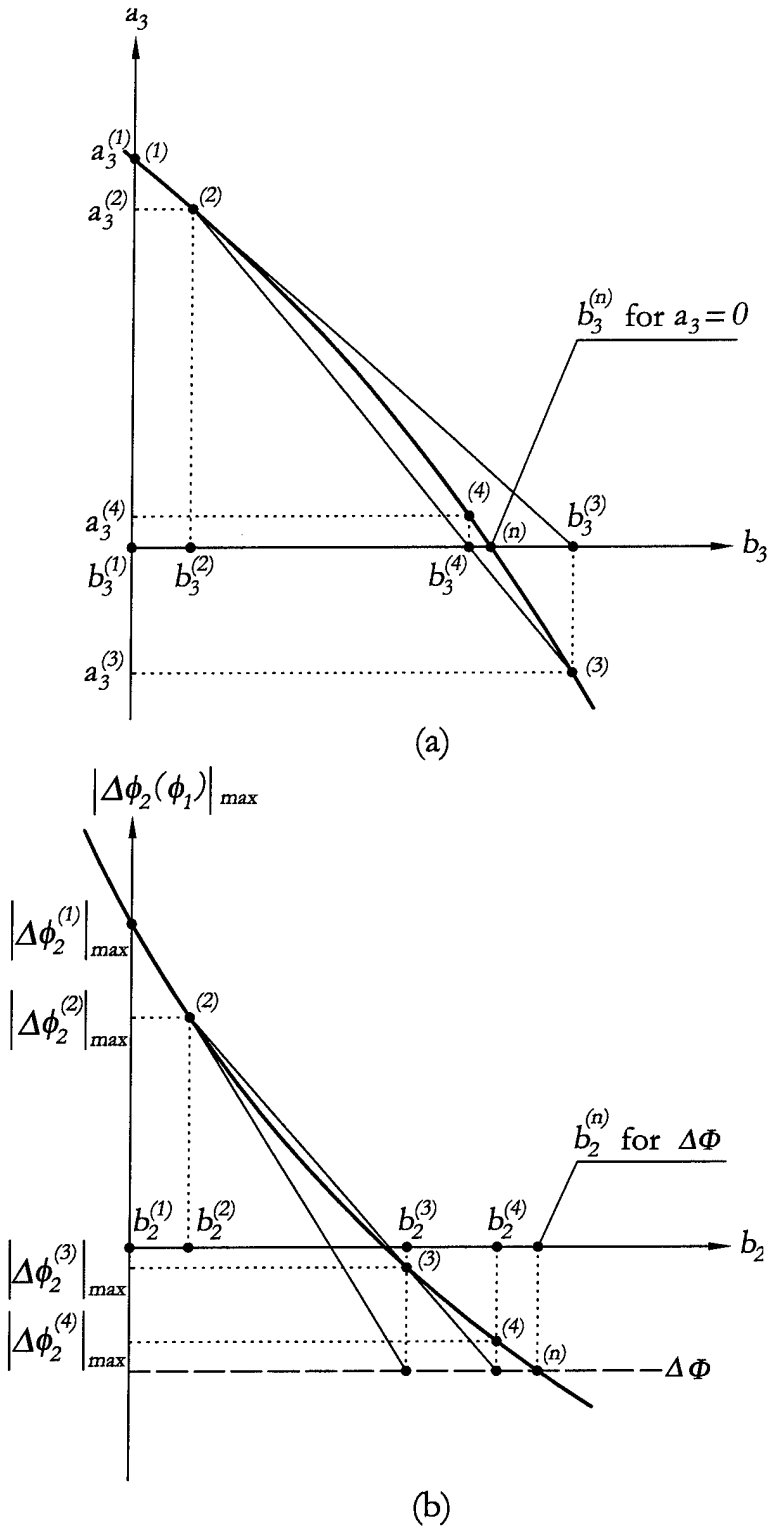

Figure 17.—Illustration of variation of coefficients b_2 and b_3 of modified roll.

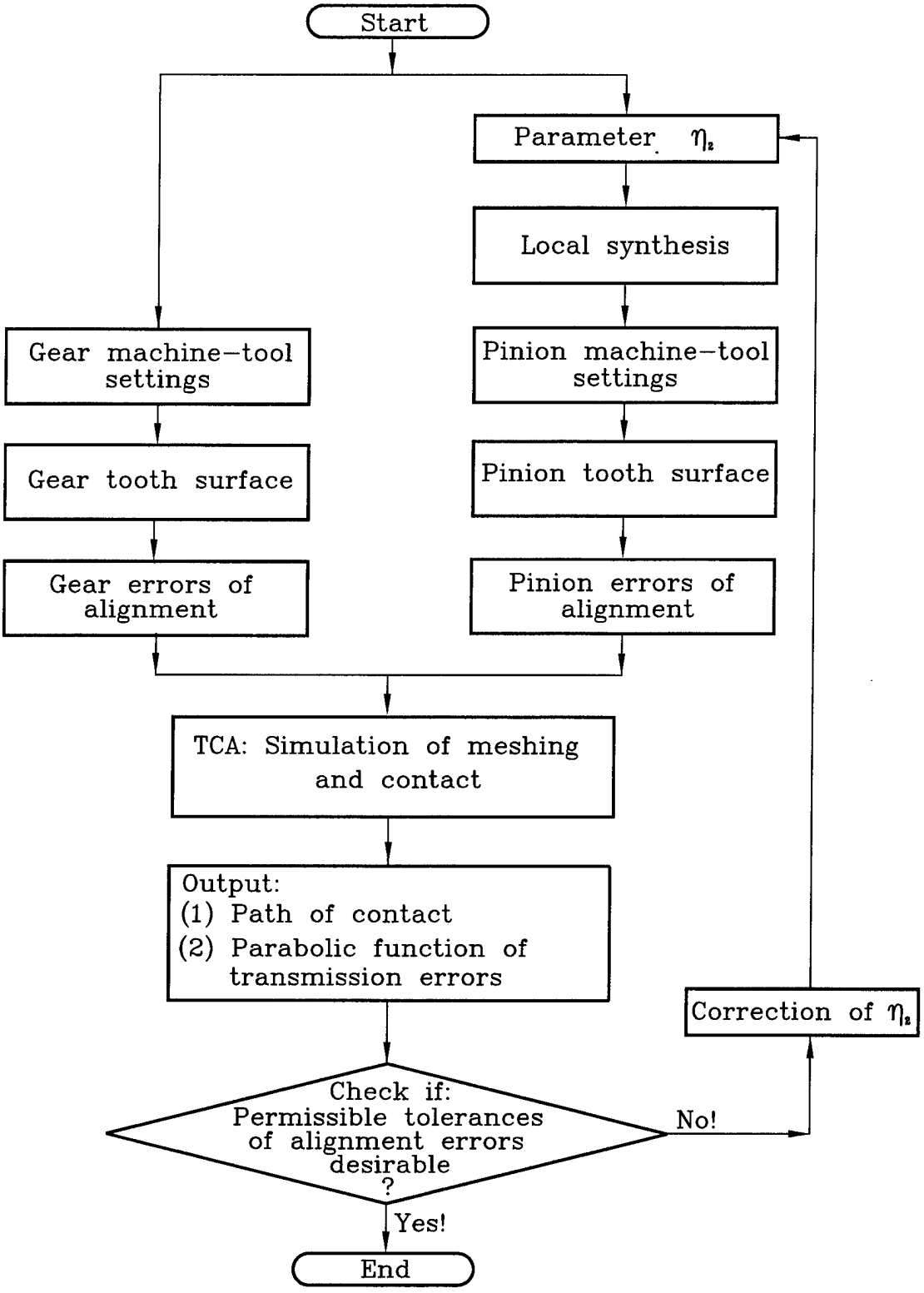

Figure 18.—Flow chart for procedure 3.

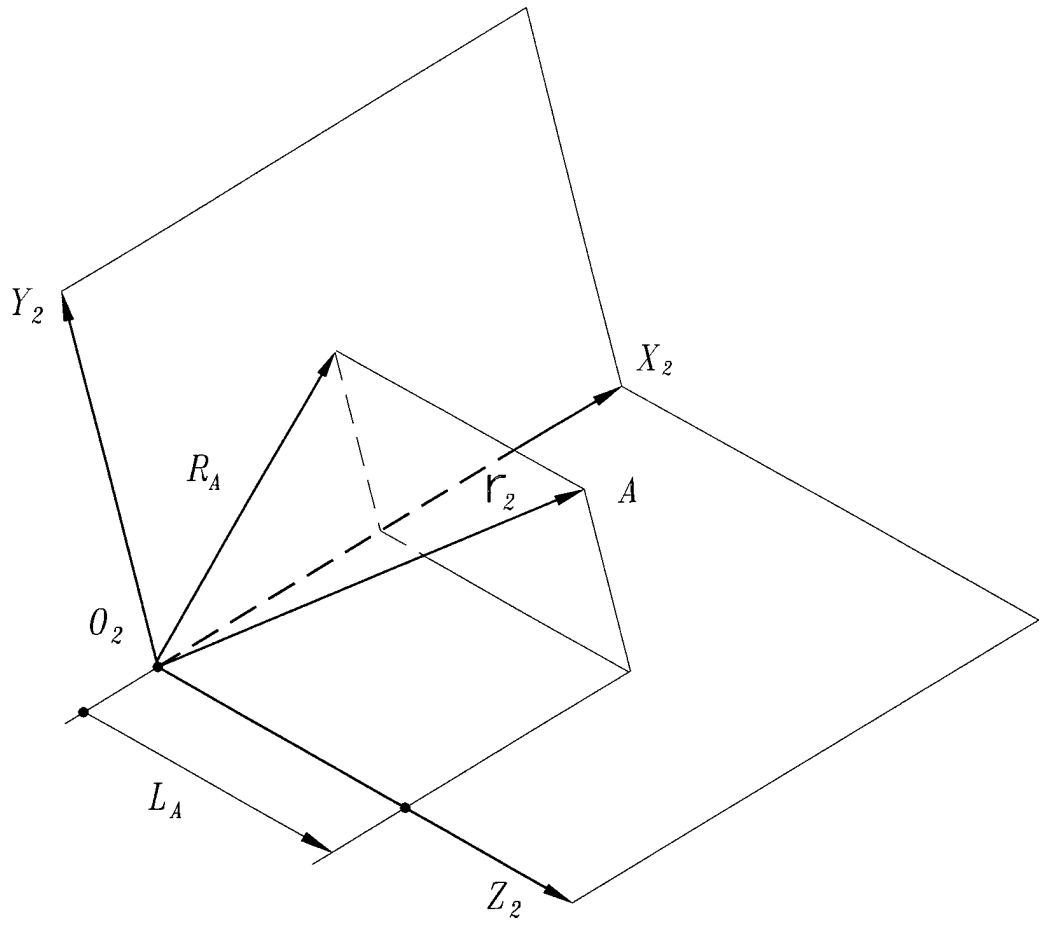

Figure 19.—Representation of point A in coordinate system S_2.

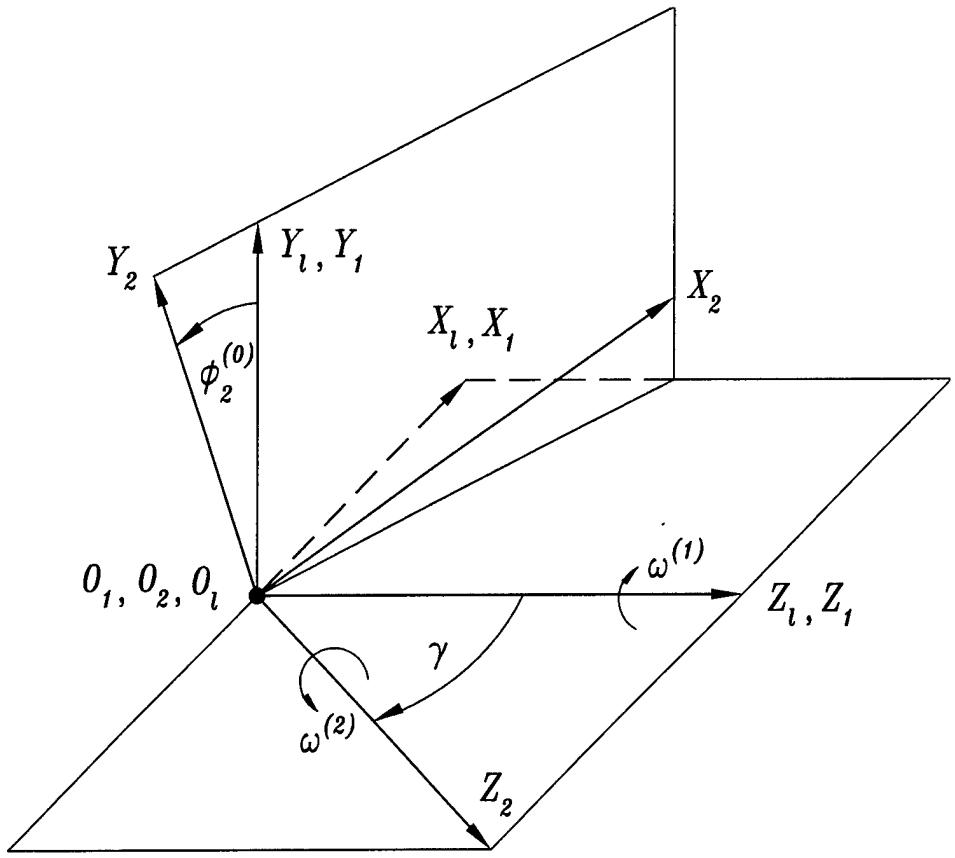

Figure 20.—Coordinate systems S_2, S_l, and S_1 applied for local synthesis.

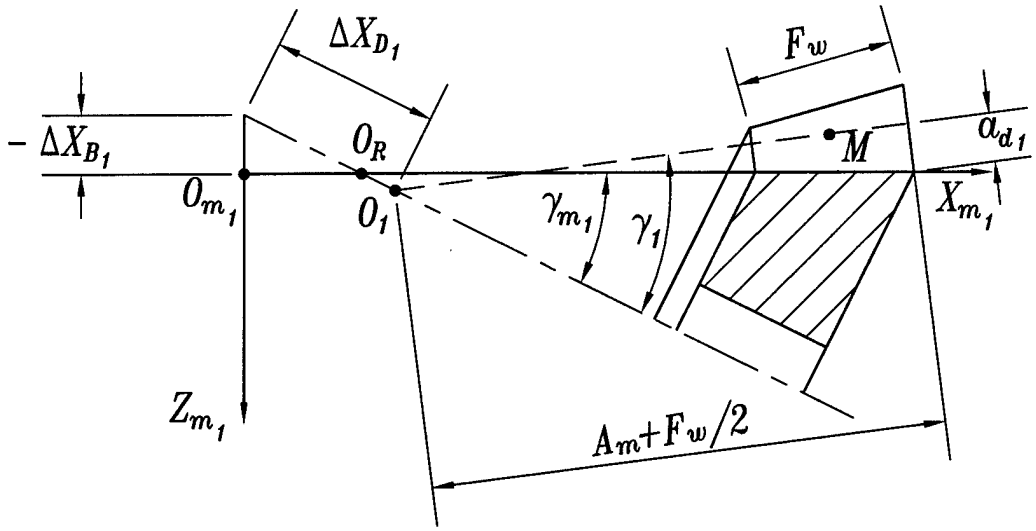

Figure 21.—For derivation of pinion machine tool settings.

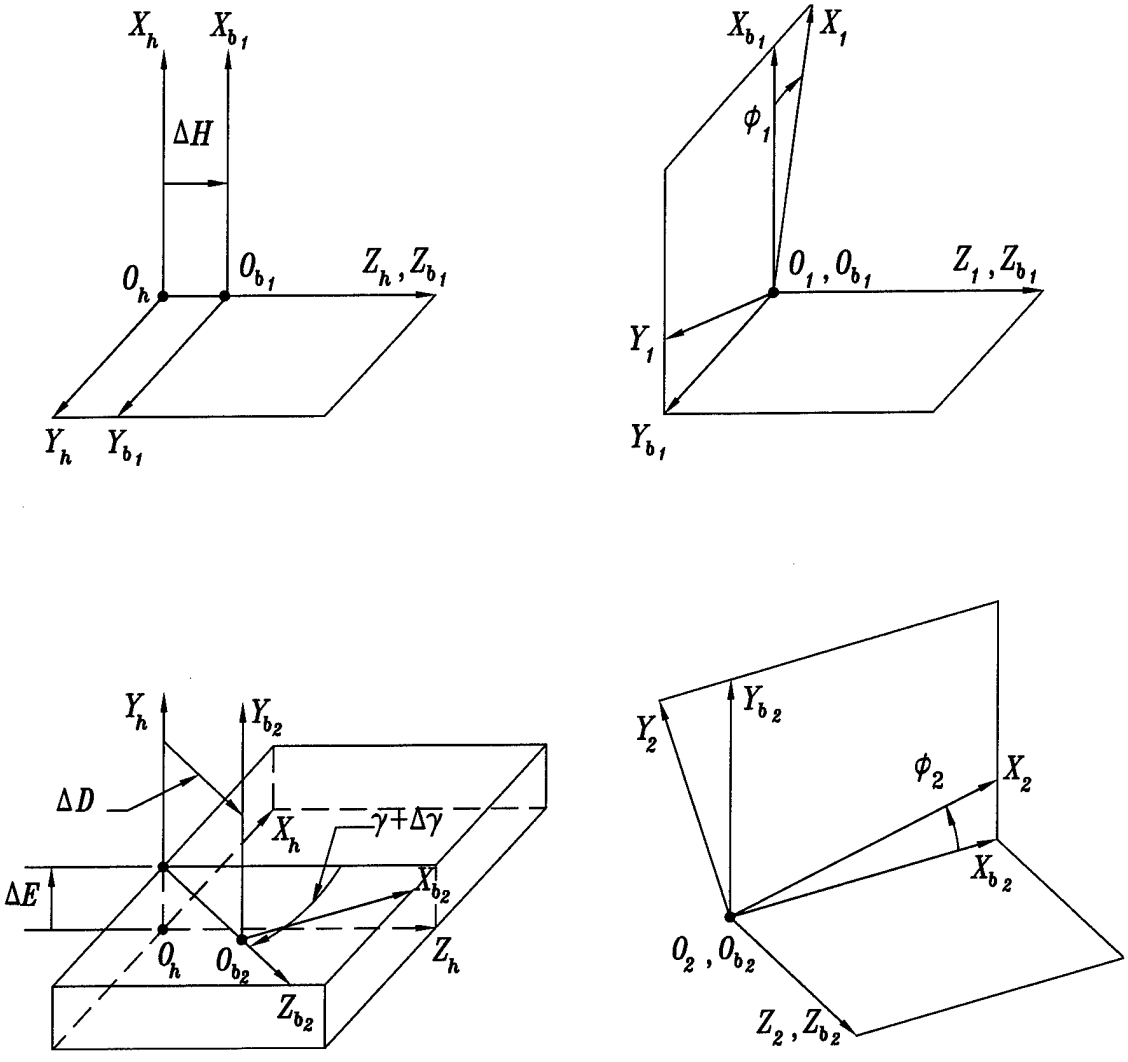

Figure 22.—Coordinate system applied for simulation of meshing of pinion and gear tooth surfaces.

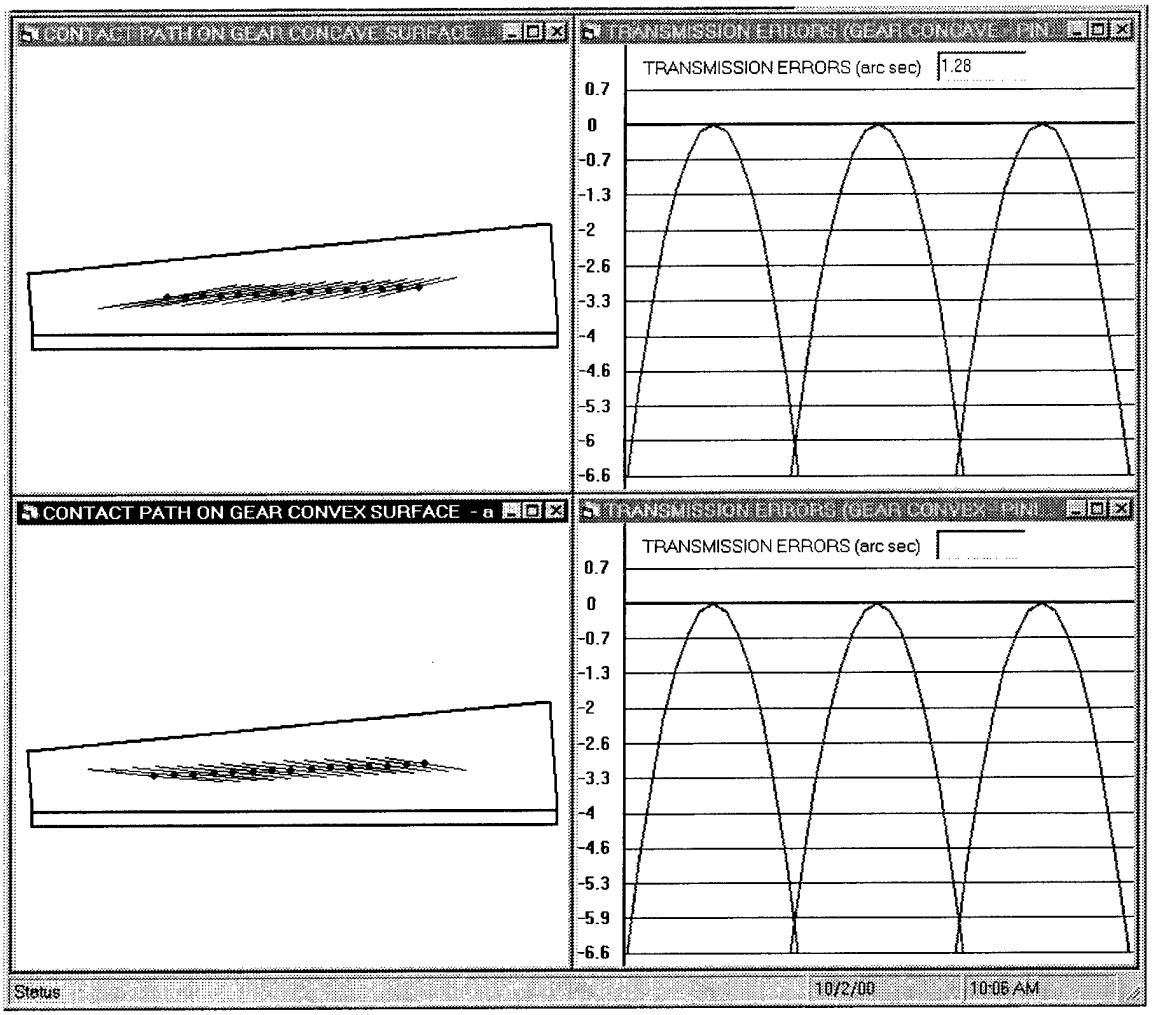

Figure 23.—TCA results output by Visual Basic: simulation of meshing without misalignment.

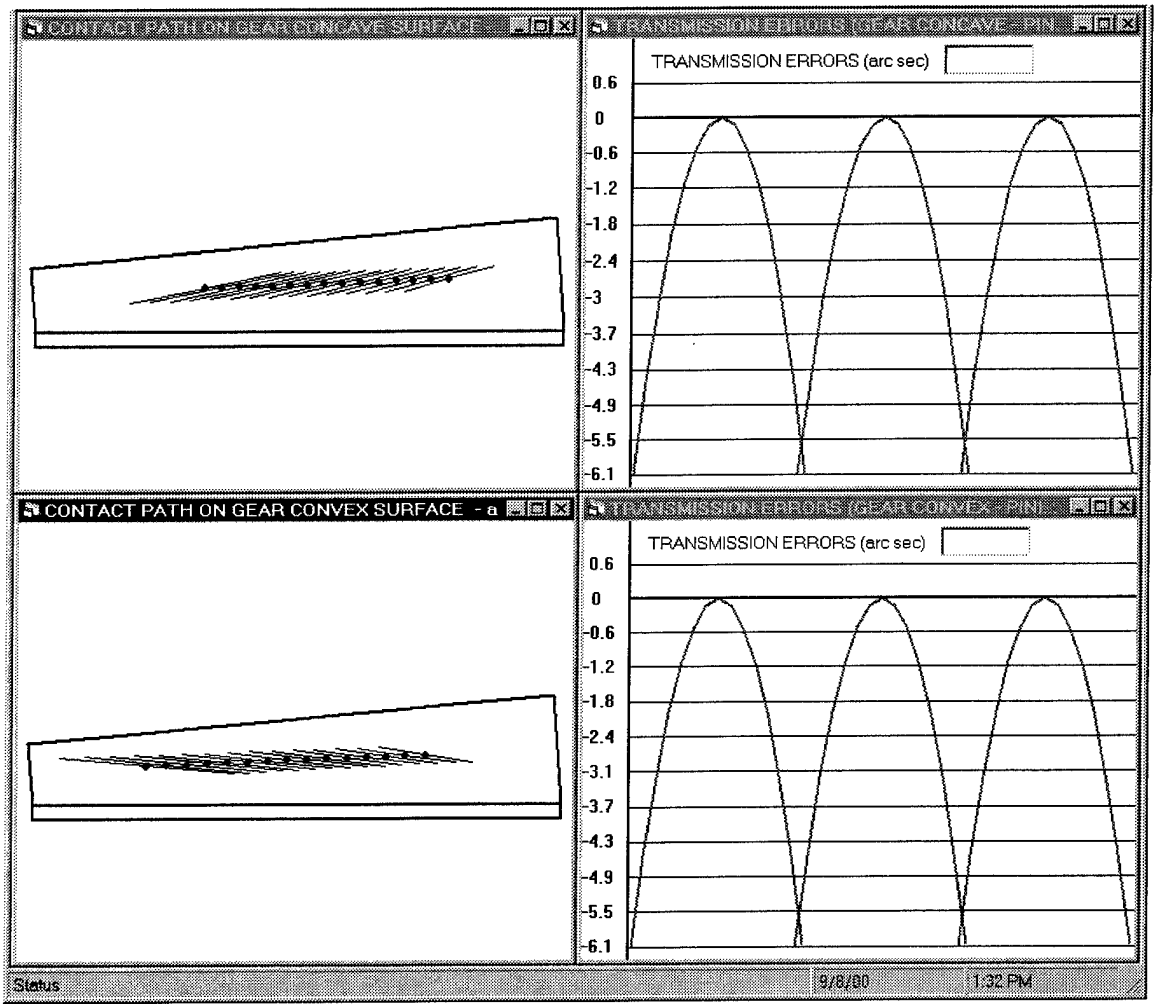

Figure 24.—TCA results output by Visual Basic: simulation of meshing with misalignment $\Delta H = 0.1$ mm.

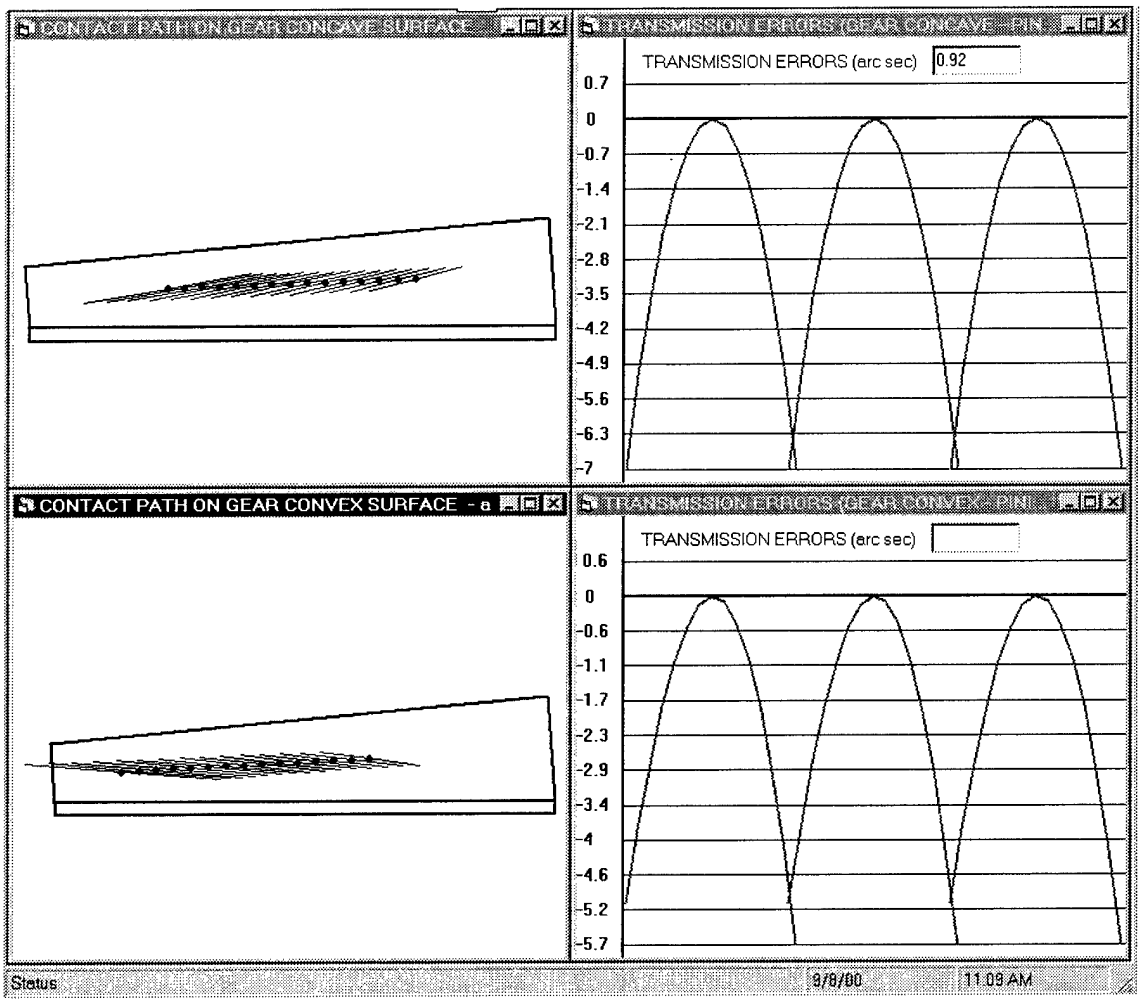

Figure 25.—TCA results output by Visual Basic: simulation of meshing with misalignment $\Delta D = 0.1$ mm.

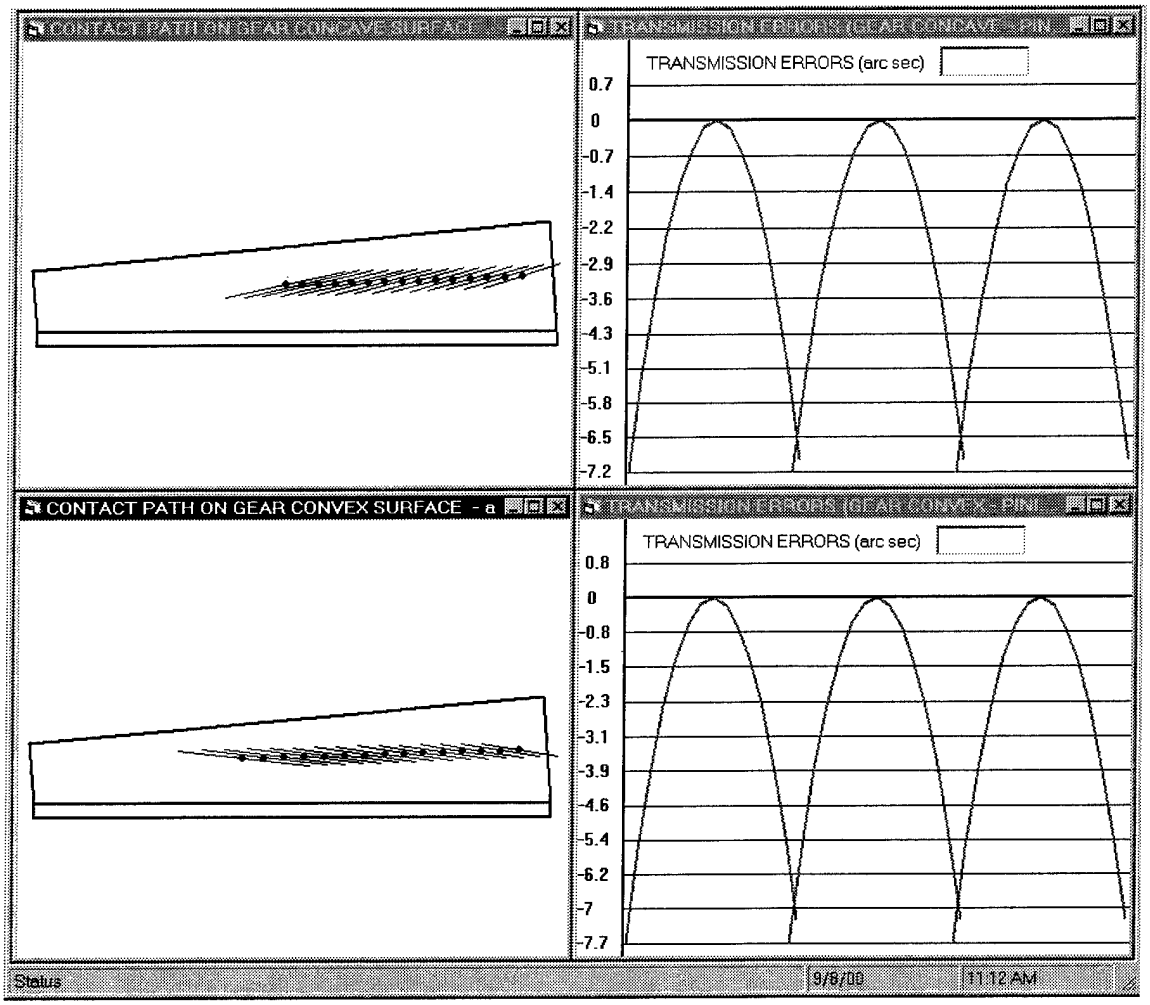

Figure 26.—TCA results output by Visual Basic: simulation of meshing with misalignment $\Delta E = 0.1$ mm.

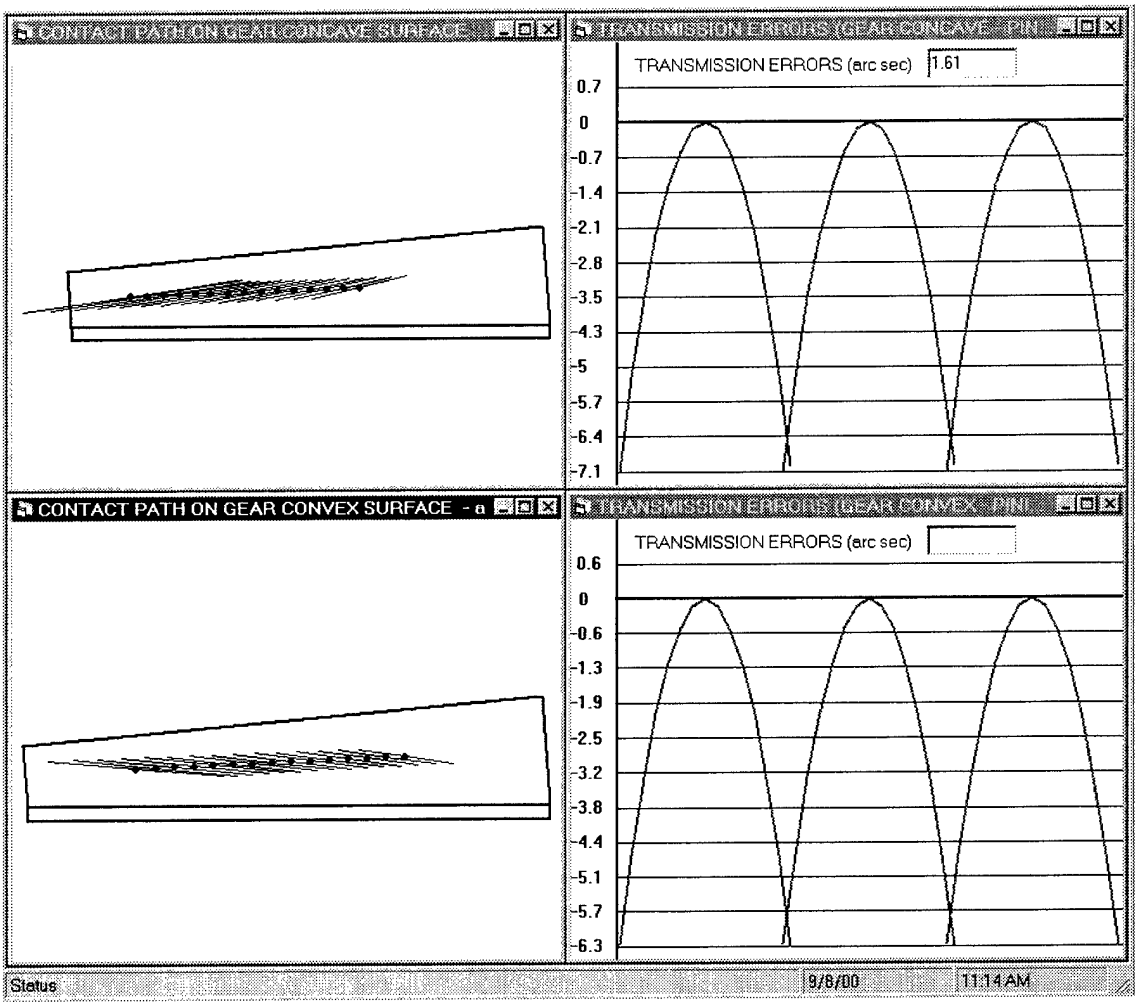

Figure 27.—TCA results output by Visual Basic: simulation of meshing with misalignment $\Delta\gamma = 3'$.

REPORT DOCUMENTATION PAGE

Form Approved
OMB No. 0704-0188

Public reporting burden for this collection of information is estimated to average 1 hour per response, including the time for reviewing instructions, searching existing data sources, gathering and maintaining the data needed, and completing and reviewing the collection of information. Send comments regarding this burden estimate or any other aspect of this collection of information, including suggestions for reducing this burden, to Washington Headquarters Services, Directorate for Information Operations and Reports, 1215 Jefferson Davis Highway, Suite 1204, Arlington, VA 22202-4302, and to the Office of Management and Budget, Paperwork Reduction Project (0704-0188), Washington, DC 20503.

1. AGENCY USE ONLY (*Leave blank*)	2. REPORT DATE	3. REPORT TYPE AND DATES COVERED
	May 2001	Final Contractor Report

4. TITLE AND SUBTITLE

Computerized Design, Generation, and Simulation of Meshing and Contact of Face-Milled Formate Cut Spiral Bevel Gears

5. FUNDING NUMBERS

WU–712–10–13–00
NAG3–2450

6. AUTHOR(S)

Faydor L. Litvin, Qi Fan, and Alfonso Fuentes

7. PERFORMING ORGANIZATION NAME(S) AND ADDRESS(ES)

University of Illinois at Chicago
Chicago, Illinois 60680

8. PERFORMING ORGANIZATION REPORT NUMBER

E–12770

9. SPONSORING/MONITORING AGENCY NAME(S) AND ADDRESS(ES)

National Aeronautics and Space Administration
Washington, DC 20546–0001
and
U.S. Army Research Laboratory
Adelphi, Maryland 20783–1145

10. SPONSORING/MONITORING AGENCY REPORT NUMBER

NASA CR—2001-210894
ARL–CR–467

11. SUPPLEMENTARY NOTES

Project Manager, Robert Handschuh, U.S. Army Research Laboratory, Structures and Acoustics Division, NASA Glenn Research Center, organization code 5950, 216–433–3969.

12a. DISTRIBUTION/AVAILABILITY STATEMENT

Unclassified - Unlimited
Subject Category: 37 Distribution: Nonstandard

Available electronically at http://gltrs.grc.nasa.gov/GLTRS

This publication is available from the NASA Center for AeroSpace Information, 301–621–0390.

12b. DISTRIBUTION CODE

13. ABSTRACT ***(Maximum 200 words)***

A new approach for design, generation, and computerized simulation of meshing and contact of face-milled, formate cut spiral bevel gears is presented. The purpose is to develop a low noise, stabilized bearing contact for this type of gear drives. The approach proposed is based on application of three procedures that permit in sequence, to provide a longitudinally directed bearing contact, a predesigned parabolic function of transmission errors and limit the shift of bearing contact caused by errors of alignment. The theory developed is illustrated with an example of design and computation.

14. SUBJECT TERMS

Gears; Transmissions

15. NUMBER OF PAGES

59

16. PRICE CODE

17. SECURITY CLASSIFICATION OF REPORT	18. SECURITY CLASSIFICATION OF THIS PAGE	19. SECURITY CLASSIFICATION OF ABSTRACT	20. LIMITATION OF ABSTRACT
Unclassified	Unclassified	Unclassified	